Topics in Current Chemistry (2020) 378:32
https://doi.org/10.1007/s41061-020-0295-7

REVIEW

Tailoring DNA Self-assembly to Build Hydrogels

Jie Chen[1,2] · Ying Zhu[1,3] · Huajie Liu[4] · Lihua Wang[1,3]

Received: 9 November 2019 / Accepted: 23 February 2020 / Published online: 7 March 2020

Abstract

DNA hydrogels are crosslinked polymeric networks in which DNA is used as the backbone or the crosslinker. These hydrogels are novel biofunctional materials that possess the biological character of DNA and the framed structure of hydrogels. Compared with other kinds of hydrogels, DNA hydrogels exhibit not only high mechanical strength and controllable morphologies but also good recognition ability, designable responsiveness, and programmability. The DNA used in this type of hydrogel acts as a building block for self-assembly or as a responsive element due to its sequence recognition ability and switchable structural transitions, respectively. In this review, we describe recent developments in the field of DNA hydrogels and discuss the role played by DNA in these hydrogels. Various synthetic strategies for and a range of applications of DNA hydrogels are detailed.

Keywords DNA nanotechnology · DNA hydrogels · Biofunctional materials · Self-assembly

Chapter 2 was originally published as Chen, J., Zhu, Y., Liu, H. & Wang, L. Topics in Current Chemistry (2020) 378: 32. https://doi.org/10.1007/s41061-020-0295-7.

✉ Huajie Liu
liuhuajie@tongji.edu.cn

✉ Lihua Wang
wanglihua@zjlab.org.cn

1 Division of Physical Biology, CAS Key Laboratory of Interfacial Physics and Technology, Shanghai Institute of Applied Physics, Chinese Academy of Sciences, Shanghai 201800, China

2 University of Chinese Academy of Sciences, Beijing 100049, China

3 Zhangjiang Laboratory, Shanghai Advanced Research Institute, Chinese Academy of Sciences, Shanghai 201210, China

4 School of Chemical Science and Engineering, Shanghai Research Institute for Intelligent Autonomous Systems, Key Laboratory of Advanced Civil Engineering Materials of Ministry of Education, Tongji University, Shanghai 200092, China

1 Introduction

Hydrogels are a class of soft materials with high water contents and three-dimensional (3D) crosslinked networks [1]. The chemical characteristics of the polymeric chains in hydrogels can be tailored to make them biocompatible and responsive to specific stimuli (e.g., heat, light, or certain molecules). Due to their unique structural and mechanical properties, hydrogels are probably the most widely used artificial materials in biomedical applications [2] such as biosensing [3], drug delivery [4], and tissue engineering [5]. Traditionally, artificial hydrogels are constructed by crosslinking hydrophilic synthetic polymers to form networks. Though the rapid growth of polymer chemistry has enabled the functionalization of hydrogels to suit specific requirements, it remains challenging to customize the structural anisotropy of hydrogels, configure their chains, and program their polymerization [5].

Linear DNA strands, which are famous for their ability to store genetic information [6], can be used as biopolymers in hydrogels, given that DNA hybridization—which obeys strict base-pairing rules—is inherently a sequence-specific self-assembly process. In 1982, Seeman suggested an unusual idea: that artificial DNA nanostructures could be created from branched DNA building blocks [7]. In such an approach, synthetic single-stranded DNAs with designed sequences recognize complementary strands and form predictable structures [8, 9]. New techniques such as DNA origami and spherical DNA have driven the rapid growth of this field in recent years [10, 11]. Similarly, programmable hybridization can lead to the random crosslinking of DNA strands in three dimensions to form hydrogels. Compared with synthetic polymer-based hydrogels, DNA hydrogels have a number of advantages, such as specific molecular recognition, multifunctionality, and excellent biocompatibility [12]. Other notable features of DNA hydrogels that can be achieved through the artful design of DNA sequences include responsiveness to multiple stimuli and tunable mechanical properties [13].

The idea of controlling sol–gel transitions using DNA can be traced back to 1987, when DNA duplexes were covalently interconnected using chemical crosslinkers for the first time [14]. Almost 10 years later, a different strategy involving the crosslinking of synthetic polymers through DNA hybridization emerged, which opened the door to hybrid DNA hydrogel synthesis [15]. However, DNA hydrogels did not attract much attention before the early 2000s, largely because nanotechnology was still in its infancy. This situation changed with the emergence of pure DNA hydrogels, as first reported by the groups of Luo and Liu [16–18]. Their creative work illustrated the infinite variety of DNA interactions that were possible (in contrast to the interactions of synthetic polymers), facilitating the synthesis of smart hydrogels. This research field has grown rapidly over the past decade [12]. Both pure and hybrid DNA hydrogels are now cutting-edge materials for next-generation biomedical and intelligent applications.

In this review, we focus on recent progress in the field of DNA hydrogels fabricated by base–base recognition mechanisms. DNA hydrogels that are formed by physical interwinding are not included in this review, but they are reviewed

elsewhere [12]. We consider different design principles and construction strategies, starting with conventional DNA hybridization strategies in which stable hydrogels are directly formed through sequence-specific hybridization. We then describe enzyme-assisted hybridization strategies and show that nonduplex DNA conformations such as i-motifs and G-quadruplexes can also form networks. Finally, we discuss emerging approaches in order to highlight the future directions for research in this field.

2 Conventional DNA Hybridization Strategies

2.1 Unbranched DNA Strands for Crosslinking Synthetic Polymers

By modifying single-stranded DNA (ssDNA) on synthetic linear polymer chains, it is possible to crosslink polymers to form 3D networks. DNA overhangs on the polymer act as side chains that can be used to connect polymers. Most hybrid DNA hydrogels are fabricated in this manner.

In 1996, Nagahara and Matsuda were the first to utilize this idea to construct a DNA–polyacrylamide hybrid hydrogel [15]. They designed two kinds of acrydite-modified single-stranded DNAs that were separately incorporated into polyacrylamide chains to obtain oligoT-polyacrylamide and oligoA-polyacrylamide. Next, they constructed two types of DNA–polyacrylamide hybrid hydrogels: one was formed by using polyA ssDNA to crosslink the oligoT-polyacrylamide (type I, Fig. 1a); the other was formed through the intermolecular crosslinking of oligoT-polyacrylamide and oligoA-polyacrylamide (type II, Fig. 1b).

To further exploit the advantages of DNA, Lin et al. demonstrated a DNA-crosslinked polyacrylamide hydrogel in which the DNA crosslinker strand incorporated a "toehold" region. Using DNA strand-displacement reactions, the crosslinks could then be eliminated through the addition of a removal strand, faciliating a

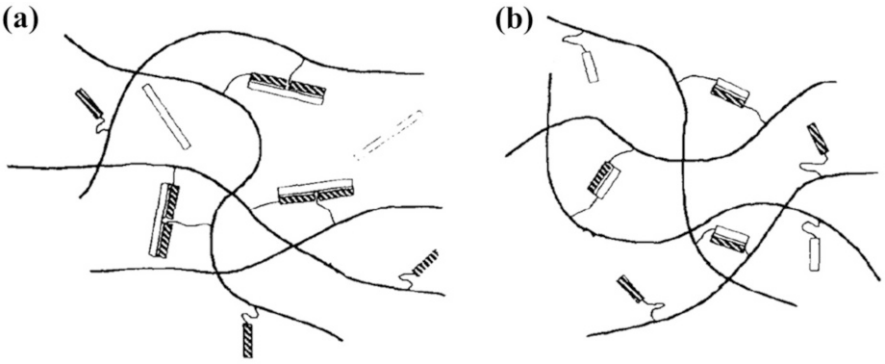

Fig. 1 DNA hydrogels formed by the hybrization of two types of single-stranded DNAs. **a** Schematic of DNA hydrogel formation through the addition of extra ssDNA to crosslink two different ssDNA-modified polymer chains. **b** Schematic of DNA hydrogel formation through the complementary hybridization of ssDNA on polymer chains. Reproduced with permission from [15]

gel-sol transition [19]. Then Lin et al. created a DNA-crosslinked hydrogel with reversible stiffness that utilized a DNA crosslinker which was designed to respond to a specific DNA "fuel" strand [20]. Moreover, Simmel and coworkers constructed a DNA-switchable gel that could be used for quantum dot delivery (Fig. 2a). The particles were released by adding DNA "release" strands that induced hydrogel delinking. The delinked gel could then be relinked by adding the crosslinking strand [21].

A series of hydrogels based on the hybridization of different types of single-stranded DNAs have been constructed and used for sensing and bioassays—for instance, in the detection of miRNAs used for clinical diagnostics. Yuan and Chai proposed a SERS platform for target miRNA detection. In the mechanism for that platform, the target miRNA induces the release of DNA via DNA displacement reactions, and the released DNA induces the dissociation of the 3D hydrogel network. This causes a Raman reporter (TB) to leak out, triggering a strong Raman signal [22]. Based on a similar principle involving a DNA hybrid hydrogel, Ding and coworkers manufactured an electrochemical biosensing platform for miR-21 detection (Fig. 2b) [23]. Li and colleagues developed a portable glucometer readout system for the detection of multiple endogenous miRNAs (Fig. 2c) [24].

Aside from schemes in which the signal is activated by the dissociation of the hydrogel, there are also schemes in which hydrogel formation induces signal enhancement or modification. Tang and colleagues designed a biosensor based on a DNA–polyacrylamide hybrid hydrogel in which Hg^{2+} activated a Mg^{2+}-specific DNAzyme that

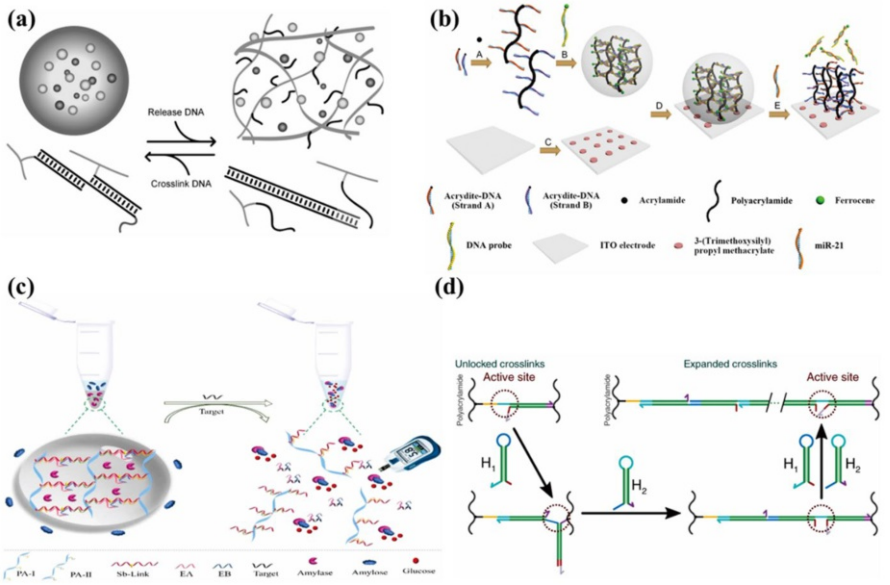

Fig. 2 Applications of DNA/RNA-responsive hydrogels. **a** Schematic of a DNA-switchable gel used for nanoparticle delivery. **b** Schematic of an electrochemical DNA hydrogel biosensor employed for the detection of miR-21. **c** Schematic of a DNA hydrogel used as a sensing platform for target miRNA detection. **d** Schematic of a DNA hydrogel that changes size upon hairpin monomer incorporation. Reproduced with permission from [21, 23, 24, 30]

produced a single-stranded DNA, which in turn initiated a hybridization chain reaction (HCR) between two hairpin-modified polymer chains that induced DNA–polyacrylamide hybrid hydrogel formation on an electrode, activating the signal [25]. Using the same principle (i.e., the initiation of a HCR between two hairpin-modified polymer chains induces the formation of a DNA hybrid hydrogel), Jie and colleagues developed a versatile DNA-hydrogel-amplified fluorescence platform for the detection of a miRNA [26]. In another scheme, the single-stranded DNA used as a crosslinker was premodified with a liposome, and this DNA-modified liposome was used to crosslink DNA-grafted polyacrylamide copolymers, yielding a DNA hydrogel [27].

Moreover, It is worth noting that until very recently, HCR was only used to form hydrogels via the crosslinking of hairpin-DNA-modified polyacrylamides [28]. However, in 2017, Schulman and colleagues designed a system in which HCR was used to successively extend the DNA crosslinker of a DNA-hybrid hydrogel with specific DNA molecules, leading to a hundredfold increase in the volume of the hydrogel [29]. Using the same hydrogel expansion mechanism, Schulman and Fern subsequently developed a new DNA-responsive system. In this system, low concentrations of biomolecular input molecules interact with molecular controllers instead of the hydrogel polymer. These molecular controllers recognize the inputs and then perform appropriate processing and amplification, leading to a strong output signal that triggers large-scale responses in the hydrogel (Fig. 2d) [30].

In all of the above schemes, the DNA strands need to interact directly with the DNA crosslinker to modify the DNA hydrogel network, as the schemes are based on strand displacement reactions. Therefore, to induce large-scale changes in the properties of the hydrogel, a high concentration of external DNA must be added to the system. To avoid this problem, Collins and coworkers exploited Cas12a, a CRISPR (clustered regularly interspaced short palindromic repeats)-associated nuclease, to actuate hydrogels crosslinked by DNA bridges. This scheme only required a low concentration of external DNA to induce changes to the hydrogel network. The mechanism used was as follows. Firstly, Cas12a binds to gRNA to form a gRNA–Cas12a complex. When the target double-stranded DNA is added, the single-stranded deoxyribonuclease (ssDNase) activity of Cas12a is activated; Cas12a indiscriminately cleaves any single-stranded DNA (ssDNA) nearby. Therefore, upon exposure to the gRNA–Cas12a and the target dsDNA, the single-stranded DNA used as the crosslinker in the hydrogel is degraded, dissociating the hydrogel network [31]. This represents a new type of DNA-responsive hydrogel based on sequence recognition of the gRNA and enzymatic cleavage of the Cas12a in the gRNA–Cas12a complex rather than strand displacement or structural changes to DNA crosslinkers. Because of the high specificity and programmability of the CRISPR-Cas12a enzyme system, this type of DNA-responsive hydrogel could be exploited as a smart drug-delivery system or diagnostic tool [32].

2.2 Pure DNA Hydrogels Based on Sticky End Complementary Hybridization

In contrast to the formation of hydrogels based on the direct hybridization of single DNA strands, another conventional DNA hybridization strategy involves the use

of branched DNA sticky end complementary hybridization. This principle has been adopted to prepare pure DNA hydrogels that only consist of whole DNA.

In 2011, Liu and coworkers created a DNA hydrogel through the sticky end complementary hybridization of two DNA building blocks (Fig. 3a). Two kinds of DNA building blocks are used in this system: Y-scaffold DNA (Y-DNA) and a DNA linker (L-DNA). The Y-DNA has three arms, each with a sticky end, and is formed through the self-assembly of three types of single-stranded DNA. The L-DNA is a linear double-stranded DNA containing two sticky ends at both ends of the DNA. The sticky ends of the L-DNA hybridize with the complementary sticky ends of the Y-DNA. The hydrogel is obtained by mixing the Y-DNA and the L-DNA in an appropriate molar ratio. It should be noted that the sticky ends of this system contrast with those of the X-DNA system created by Luo [16], in which the sticky ends are palindromic sequences. Instead, in the system designed by Liu and coworkers, palindromic sequences are avoided as much as possible to suppress self-linking. Therefore, the resulting DNA hydrogel is homogeneous. The thermal response of this DNA hydrogel is dependent on the length and the composition of the sticky ends [18]. Including restriction sites on the L-DNA allows it to be cleaved by the corresponding restriction enzyme, leading to the disruption of the hydrogel network. Thus, this enzyme-triggered DNA hydrogel could be used to envelop and then, when triggered, release single cells (Fig. 3b) [33]. A series of DNA hydrogels

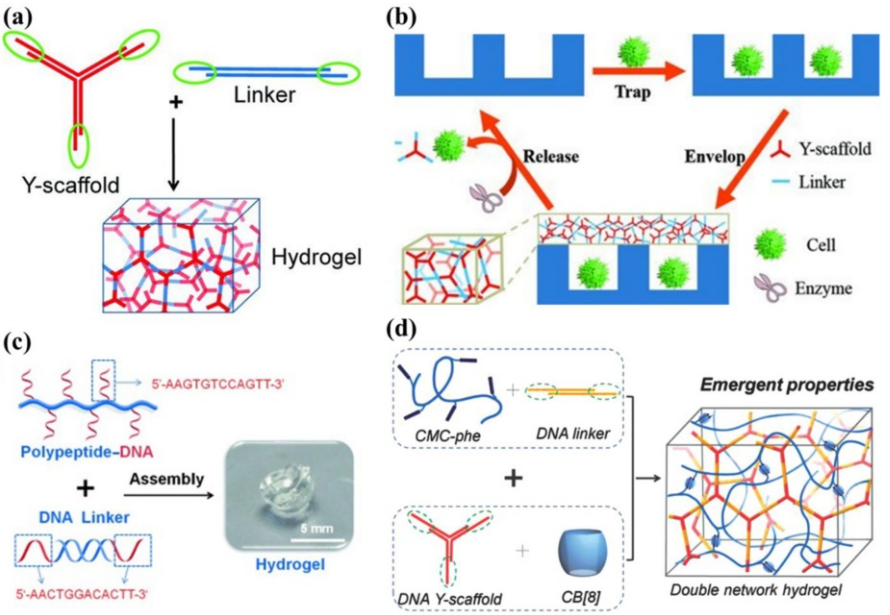

Fig. 3 DNA hydrogel schemes based on sticky end complementary hybridization, and some applications of them. **a** Schematic of DNA hydrogel formation via Y-scaffold and linker self-assembly. **b** Schematic of a DNA hydrogel that dissociates in response to a specific restriction enzyme; this hydrogel could be used to envelop and (when triggered) release cells. **c** Schematic of polypeptide-DNA hydrogel formation through the hybridization of the sticky ends in the DNA linker with the ssDNA on the polypeptide. **d** Schematic of a double-network hydrogel. Reproduced with permission from [18, 33, 35, 36]

based on the same strategy were then reported by Liu's group. For example, a new type of DNA–polypeptide hydrogel was developed [34]. After a series of improvements, they created a supramolecular polypeptide-DNA hydrogel that could be used as a bioink in 3D bioprinting (Fig. 3c) [35]. In addition, responsive double-network (i.e., dual crosslinked) hydrogels were constructed based on cucurbit[8]uril hydrogel networks (Fig. 3d) [36]. A DNA hydrogel with modifiable macroscopic mechanical properties was prepared using an i-motif sequence in the linear linker [37], a hydrogel based on DNA-modified magnetic nanoparticles was created [38], and a tissue-like DNA supramolecular hydrogel permitting cell migration was fabricated [39]. A polypeptide-DNA supramolecular hydrogel with rheological properties that could be modified without changing the network topology and crosslinker was also developed [40]. Moreover, the microrheology of a DNA hydrogel formed from Y-shaped DNA building blocks was studied in detail using diffusing-wave spectroscopy (DWS) [41].

An X-shaped DNA crosslinker with four arms that have sticky ends was designed for the fabrication of multifunctional hydrogels in 2015 (Fig. 4a). To prepare this X-shaped DNA linker, two kinds of Y-shaped DNA were prepared through the self-assembly of two groups of three types of single-stranded DNA, respectively. Upon mixing the two kinds of Y-shaped DNA equally, they assembled to form the X-shaped DNA crosslinker. Two of the arms of the X-shaped DNA serve as crosslinking sites, while the other two are free sticky ends that can be used for further modifications through precise DNA hybridization. Therefore, different functional groups can be attached to the hydrogel network in a specified ratio via reliable DNA hybridization [42]. Using this multiarm DNA crosslinker, Ignatius and coworkers reported the preparation of a multifunctional DNA–protein hybrid hydrogel from modified human serum albumin. The specific multicomponent loading of this

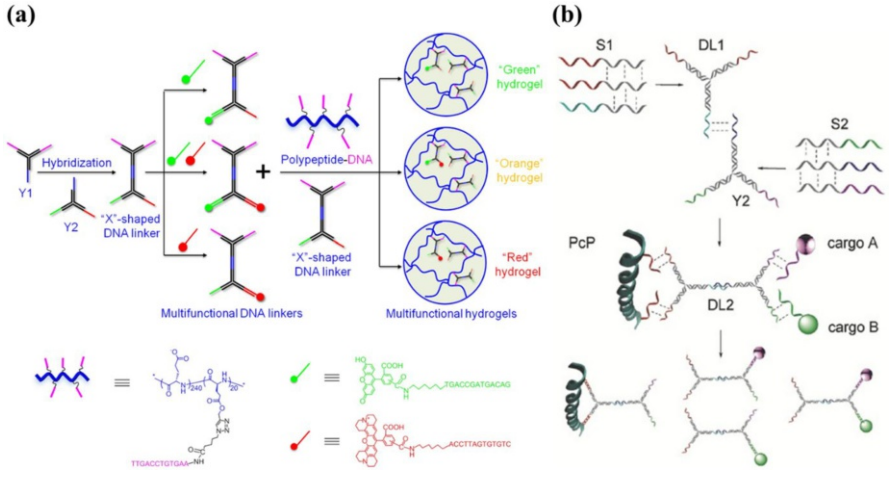

Fig. 4 X-shaped DNA used as a multiarm DNA crosslinker for DNA hydrogel formation. **a** Schematic of the use of rationally designed multifunctional DNA linkers to construct a multifunctional polypeptide-DNA hydrogel. **b** Schematic of the preparation of a protein-DNA hydrogel that is capable of loading and releasing multifunctional cargos. Reproduced with permission from [42, 43]

hydrogel with bioactive cargos and the spatiotemporally controlled release of those cargos from the hydrogel were demonstrated (Fig. 4b) [43].

Moreover, using the Y-DNA and L-DNA model for DNA hydrogel construction, Willner and colleagues demonstrated a Y-shaped DNA structure that was modified with Ag nanoclusters (Ag-NCs) at a specific loop domain in the Y-scaffold. Addition of a DNA linker resulted in the crosslinking of the Y-scaffold to form a three-dimensional hydrogel network containing fluorescent Ag-NCs [44]. Minteer and colleagues used a similar approach to entrap glucose oxidase in a DNA hydrogel, thus producing an enzymatic biobattery [45]. Later, they constructed DNA redox hydrogels by coimmobilizing redox mediators and glucose oxidoreductase enzymes in DNA hydrogels [46]. Similar hydrogels could also be used directly for biotherapy without the need for any chemical modification. For instance, DNA hydrogels in which the linear linker bears unmethylated cytosine-phosphate-guanine (CpG) dinucleotides can be used for tumor vaccinations [47]. This type of hydrogel could also be applied as an ophthalmic therapeutic delivery system [48].

There are other DNA hydrogel design strategies based on sticky end complementary hybridization too. For instance, Takakura and Nishikawa reported a self-gelling and injectable DNA hydrogel based on polypod-like DNA (polypodna) that self-assembled under physiological conditions. This concept was used to create a DNA hydrogel bearing unmethylated cytosine-phosphate-guanine (CpG) dinucleotides that could be used to stimulate innate immunity [49]. Afterwards, Nishikawa employed this method to construct a series of DNA hydrogels for biotherapy. Among them, Nishikawa and coworkers developed a Takumi-based DNA hydrogel (Fig. 5a) [50]. In order to further expand the applications of this hydrogel and improve its therapeutic effects, the hydrogel was mixed with chitosan to improve its sustained release characteristics [51]. Oral delivery of CpG DNA was achieved by coating the hydrogel with chitosan [52]. An enhanced immune response was realized by generating a hydrogel incorporating cholesterol-modified DNA [53]. They also achieved

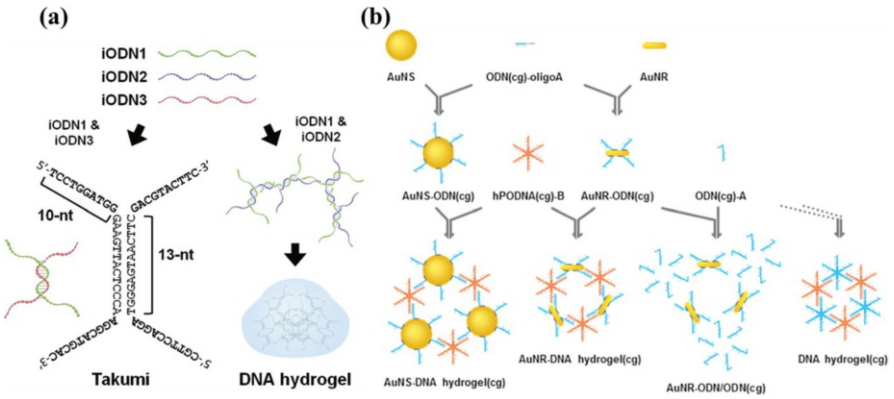

Fig. 5 DNA hydrogels formed through the self-assembly of polypod-like DNA (polypodna). **a** Schematic of the formation of Takumi and a Takumi-based DNA hydrogel. **b** Schematic of the synthesis of AuNS-DNA and AuNR-DNA hydrogels based on hexapodna self-assembly. Reproduced with permission from [50, 54]

a composite-type immunostimulatory DNA hydrogel by mixing appropriately designed hexapod-like DNA (hexapodna)-bearing CpG sequences with oligodeoxynucleotide-modified gold nanoparticles (Fig. 5b). When the hydrogel was irradiated with laser light, hexapodna was released, which stimulated immune cells with its CpG sequences [54]. Filetici and Francesco reported a re-entrant DNA hydrogel based on tetravalent DNA nanostars [55]. They systematically characterized the viscosity and the linear viscoelastic moduli for two different tetravalent DNA nanostar hydrogels [56]. In addition, the relationship between the structure of the tetravalent DNA nanostar hydrogel and its nonequilibrium dynamics was explored [57]. Kelley used a DNA three-way junction (TWJ) nanostructure and DNA-templated quantum dots (QDs) to construct a self-assembled quantum dot DNA hydrogel [58]. A gold nanoparticle (NP) DNA hydrogel based on a DNA three-way junction nanostructure was also developed [59]. Ding constructed a DNA hydrogel with two kinds of X-shaped DNA polymers: 1 and 2. When the two X-shaped DNA polymers were mixed, complementary hybridization of their sticky ends occurred, yielding the DNA hydrogel [60].

As well as schemes that use complex DNA-based systems, short linear double-stranded DNA (dsDNA) equipped with sticky ends has also been used as a building block to form hydrogels (Fig. 6a) [61]. A thermoresponsive DNA hydrogel was used to monitor the diffusion of guest molecules [62]. In a slightly different system, short linear double-stranded DNA (dsDNA) equipped with sticky ends was used to crosslink the main chains of a hydrogel, which were long linear double-stranded DNAs. Therefore, the determinant of hydrogel formation was the crosslinking strand (Fig. 6b, c) [63]. Adopting a similar strategy, Nakatani developed a specific DNA-strand-responsive DNA hydrogel based on a well-designed DNA circuit. The sol–gel phase transition of the DNA hydrogel was realized by adding different DNA strands (Fig. 6d) [64].

Moreover, in contrast to schemes that require multiple types of single-stranded DNA, it is also possible to use just one kind of DNA to construct a DNA hydrogel. Such one-strand (OS) hydrogels can be created using a single DNA strand with multiple domains, where each domain is a self-complementary palindromic sequence. The hydrogel is then formed in a single-step process in which individual strands are crosslinked together by the complementary domains (Fig. 6e). This DNA hydrogel formation method is simple and programmable [65].

3 DNA Hydrogels Formed Using Enzymes

3.1 DNA Hydrogels Formed Using Ligase

Adopting conventional DNA hybridization strategies to construct DNA hydrogels requires sufficiently long sticky ends to stabilize the crosslinker. Ligase can join DNA fragments with complementary sticky ends and can repair nicks in double-stranded DNA with 3′-hydroxyl and 5′-phosphate ends. Therefore, ligase can be used to covalently crosslink such DNA with complementary sticky ends to form hydrogels. In 2006, Luo and coworkers reported that a pure DNA hydrogel had been

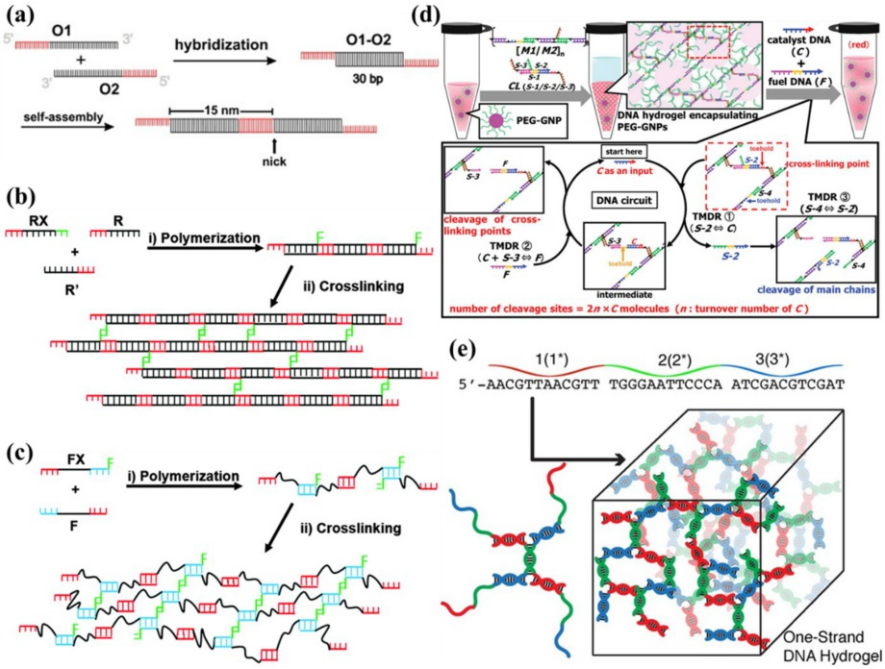

Fig. 6 DNA hydrogels formed via short dsDNA or one-stranded ssDNA self-assembly. **a** Schematic of a hydrogel formed by short linear double-stranded DNA self-assembly. **b** Schematic of a hydrogel formed by the hybridization of sticky ends, leading to rigid double-helix DNA chain crosslinking. **c** Schematic of a hydrogel formed by the hybrization of sticky ends, leading to the crosslinking of flexible DNA chains bearing ssDNA segments. **d** An artfully designed DNA circuit system that was used to create a dynamically programmed DNA hydrogel. **e** Schematic of a hydrogel formed through one-strand DNA self-assembly. Reproduced with permission from [61, 63–65]

constructed entirely from branched DNA for the first time. To obtain this pure DNA hydrogel, the authors designed and synthesized three types of branched DNA monomers: X-DNA, Y-DNA, and T-DNA. Each arm of these branched DNA monomers was a complementary sticky end containing palindromic sequences. Thus, due to the presence of the self-complementary sticky ends, the branched DNA monomers could be assembled via subsequent ligation with T4 DNA ligase into large-scale 3D-structured DNA hydrogels. The authors found that the X-DNA-based hydrogel had better mechanical properties, was more resistant to degradation, and exhibited better sustained release characteristics than the Y-DNA-based hydrogel and the T-DNA-based hydrogel [16].

Subsequently, Luo's group invented a cell-free protein-producing hydrogel system by incorporating actual plasmid DNA genes into a hydrogel. Similarly to the X-DNA hydrogel system mentioned above, this hydrogel was constructed by mixing X-DNA and linear plasmids in a predetermined molar ratio and then applying T4 DNA ligase to form the hydrogel for protein expression [66]. They then scaled up this protein-producing hydrogel by combining it with microfluidic devices, which

resulted in a high generation rate [67]. A similar method can be used to create a hydrogel for mRNA generation. Um and coworkers created a pseudo-eukaryotic nucleus (PEN) which contained a DNA hydrogel that was formed using a target gene with X-shaped DNA via ligation performed by T4 DNA ligase (Fig. 7a). When taken up by a cell, the hydrogel generated mRNA transcripts for protein translation [68]. Moreover, a similar approach was used to create a nanoscale DNA hydrogel that was constructed to produce siRNA and interfere with protein expression in a cell (Fig. 7b) [69]. In addition to using it to integrate a target gene in order to produce proteins and RNA, Takakura and Nishikawa used the sole X-DNA hydrogel system model to develop a highly immunostimulatory DNA hydrogel by connecting X-DNA incorporating six highly potent unmethylated cytosine-phosphate-guanine (CpG) dinucleotide motifs using T4 DNA ligase. They found that this CpG DNA hydrogel was an ideal system for drug delivery [70]. In 2015, Park assembled gold nanoparticles (AuNPs) in a nanoscale DNA hydrogel (Fig. 7c), generating a carrier for anticancer drugs such as doxorubicin (Dox). When excited by near-infrared (NIR) laser light, the AuNPs in the DNA hydrogel generate heat due to the photothermal effect, leading to the disintegration of the DNA hydrogel network through thermal denaturation and the release of the Dox. Thus, a DNA hydrogel permitting photo-thermo-chemo combination therapy was realized [71]. A similar strategy was also achieved using gold nanorods (AuNRs) [72]. Other applications of this hydrogel formation model have also been reported. For instance, nano/microscale DNA

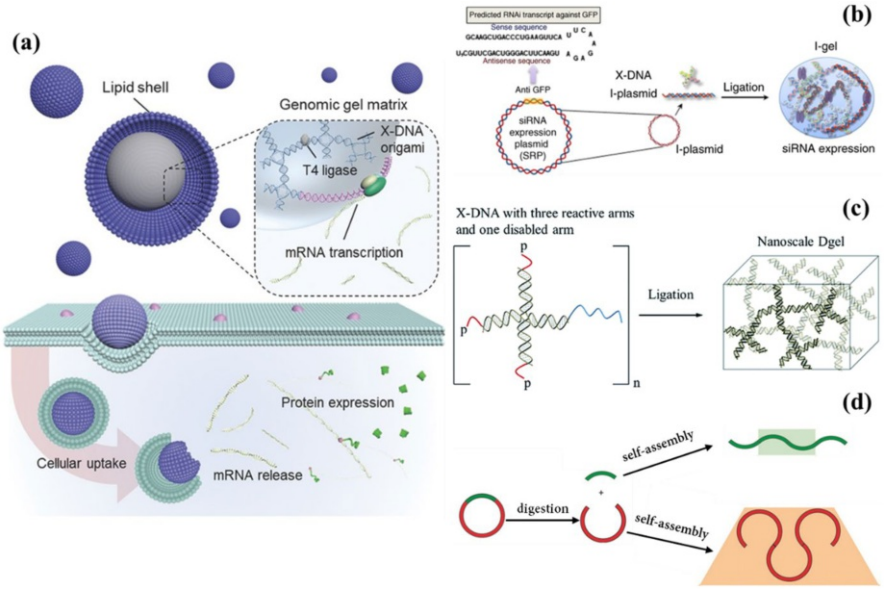

Fig. 7 DNA hydrogels formed with the assistance of ligase. **a** Schematic of a gene-containing DNA hydrogel in a pseudo-eukaryotic nucleus (PEN) for mRNA transcription. **b** Schematic of the principle of a DNA hydrogel used for RNA interference. **c** Schematic of the construction of a nanoscale DNA hydrogel. **d** Schematic of the formation of a DNA hydrogel from the plasmid pUC19. Reproduced with permission from [16, 69, 71, 77]

hydrogels were fabricated in lipid strata [73] and in multi-inlet microfluidic channels [74]. In addition, a nanostructured DNA hydrogel was used as a template to prepare an energy storage device [75] and a supercapacitor electrode [76].

Linear double-stranded DNA obtained from plasmid DNA by enzymatic digestion is also a desirable DNA building block for DNA hydrogels. In this case, hydrogel formation is achieved via the formation of covalent bonds between individual building blocks during enzymatic ligation. The plasmid pUC19 was cleaved by two kinds of endonuclease, yielding two fragments—two types of linear double-stranded DNA with sticky ends containing self-complementary palindromic sequences. These two fragments were separated and then used to form a DNA hydrogel under the direction of the ligase (Fig. 7d) [77].

3.2 DNA Hydrogels Formed Using Polymerase

Polymerase chain reaction (PCR) products that self-assemble to form DNA hydrogels can be realized through the rational design of primer sequences. Luo and colleagues performed PCR using psoralen-crosslinked thermostable Y-shaped DNA as a primer to generate a DNA hydrogel. Because the Y-shaped DNA branches maintained their branched structure during the PCR, they could be used as crosslinking points during hydrogel fabrication (Fig. 8a) [78]. In 2017, Romesberg and coworkers developed bottlebrush primers constructed from 2′-azido-A DNA, alkyne-pUC-F (forward DNA primer), and alkyne-pUC-R (reverse DNA primer) using a chemical click reaction. They then applied DNA polymerase and the bottlebrush primers in a PCR to amplify pUC19, which resulted in a DNA hydrogel (Fig. 8b) [79].

Another polymerase can be used to facilitate DNA self-assembly into hydrogels. That polymerase is terminal deoxynucleotidyl transferase (TdT), which catalyzes the repetitive addition of dNTP to the 3′-OH ends of a primer without the need for a template [80]. An X-shaped DNA motif was used as the primer to produce a hydrogel. This X-shaped DNA motif can elongate in four directions, and X-shaped DNA motifs with poly-A and poly-T tails can be obtained by adding dATP and dTTP, respectively. The hydrogel was formed by hybridizing the X-shaped DNA motifs with poly-T and poly-A tails (Fig. 8c) [81, 82].

4 DNA Hydrogels Based on Special DNA Structures

4.1 DNA Hydrogels Based on an i-Motif or DNA Triplex

i-motifs are pH-sensitive DNA structures that can be obtained by folding cytosine-rich strands in an acidic environment [13]. In 2009, Liu and coworkers invented a pure DNA hydrogel that was formed by directly inducing crosslinking between i-motif structures (Fig. 9a). To construct this hydrogel, Y-shaped DNA was first prepared from three types of single-stranded DNAs. Each arm of the resulting Y-shaped DNA included interlocking domains that enabled the generation of intermolecular i-motif structures. In an alkaline environment, the interlocking

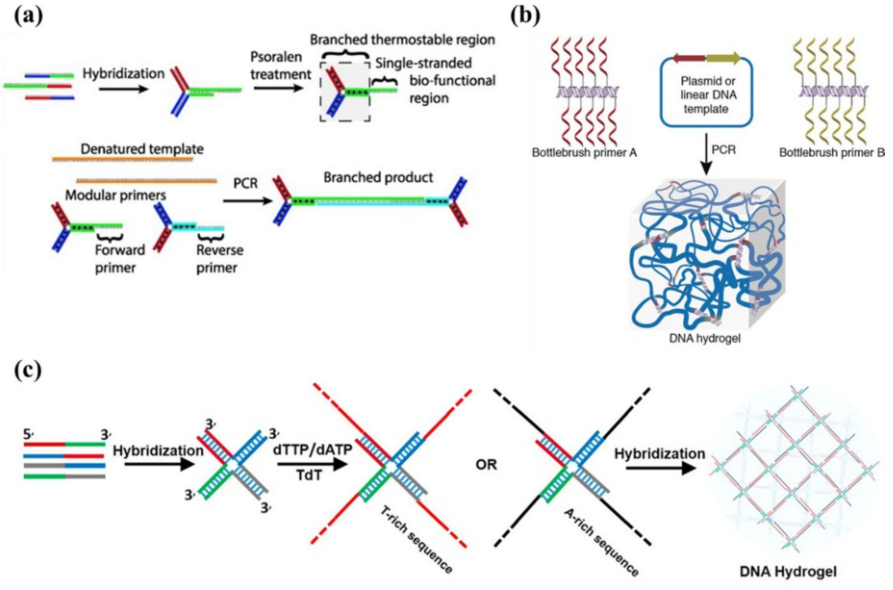

Fig. 8 DNA hydrogels formed with the assistance of polymerase. **a** Schematic of hydrogel formation using PCR with branched thermostable DNA primers. **b** Schematic of hydrogel formation via PCR using bottlebrush primers. **c** Schematic of hydrogel formation through the self-assembly of two kinds of X-shaped DNA motifs with poly-T and poly-A tails by terminal deoxynucleotidyl transferase (TdT). The tails were added to the X-shaped DNA motif in a previous step. Reproduced with permission from [78, 79, 81]

domains are configured as random coils due to electrostatic repulsion, leading to isolated Y-shaped DNA structures. Upon increasing the pH to 5.0, intermolecular i-motif structures form due to interactions of protonated cytosines with unprotonated cytosines. There were only the inter-Y-shaped i-motif structures because of the rational design. This DNA hydrogel was generated rapidly and exhibited high crosslinking density [17]. Liu and coworkers used an i-motif structure to prepare a hybrid DNA–single-walled carbon nanotube (SWNT) hydrogel in 2011 (Fig. 9b) [83]. Afterwards, Willner reported a pH-dependent dual-response DNA–pNIPAM hybrid hydrogel in which an i-motif was the pH-responsive unit (Fig. 9c). To construct this pH-triggered DNA–pNIPAM hybrid hydrogel, an acrylamide monomer modified with a cytosine-rich oligonucleotide was polymerized with *N*-isopropylacrylamide (NIPAM) monomer to obtain a hybrid copolymer with cytosine-rich sequences. When the pH was 5.2, the cytosine-rich sequences self-assembled into an i-motif structure that crosslinked the hybrid copolymer, leading to the formation of a hydrogel. When the pH was increased to 7.5, the i-motif structure and therefore the hydrogel disassembled. Due to the temperature sensitivity of pNIPAM, this hydrogel was found to respond to changes in both pH and temperature [84]. Because of their sensitivity to pH, i-motifs have been widely used in shape-memory hydrogels [85, 86]. In addition, in 2017, a hydrogel was generated using a linear DNA with half an i-motif sequence at both ends [87]. In a similar method, a single-stranded DNA with

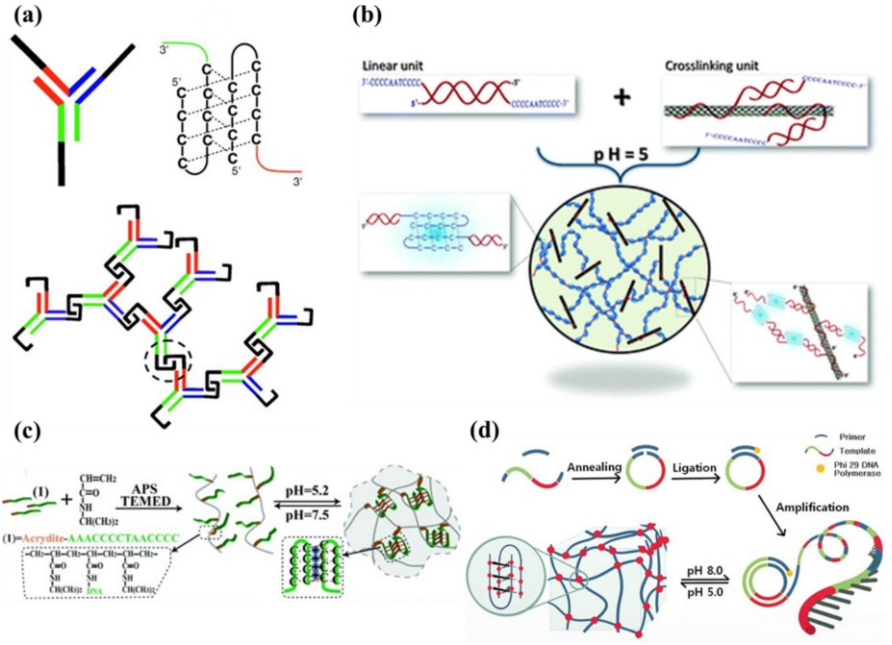

Fig. 9 DNA hydrogel formation based on i-motifs. **a** Schematic of DNA hydrogel formation based on an intramolecular i-motif. **b** Schematic of the formation of a DNA–SWNT hybrid hydrogel. **c** Schematic of the synthesis of a DNA–pNIPAM hybrid hydrogel that exhibits pH-controlled formation and dissociation. **d** Schematic of the self-assembly of RCA products with intermolecular i-motifs into a hydrogel. Reproduced with permission from [17, 83, 84, 89]

two self-complementary sequences and half an i-motif sequence was used to prepare a hydrogel [88]. Moreover, using appropriate design templates, RCA products containing intermolecular i-motifs were realized and used to form hydrogels under acidic conditions (Fig. 9d) [89].

Just like i-motifs, DNA triplexes are sensitive to pH. DNA triplexes are formed through Hoogsteen base pair interactions. Under acidic conditions, Hoogsteen base interactions mainly appear as $CG{\cdot}C^{+}$ domains, whereas, under neutral pH conditions, appear as TA·T parallel domains. In 2015, Willner was the first to use a triplex DNA structure as a crosslinker in the construction of a pH-responsive DNA hybrid hydrogel (Fig. 10a) [90]. DNA triplexes were then used by Willner's research group to prepare a shape-memory hydrogel (Fig. 10b, c) [91–93]. They have also been used to construct pH-activated pure DNA hydrogels (Fig. 10d) [94].

4.2 DNA Hydrogels Based on G-Quadruplexes

G-quadruplexes are the result of self-assembly by guanine (G)-rich nucleic acid sequences in the presence of ions (K^{+}, Pb^{2+}, or NH^{4+}). Willner was the first to construct a DNA–polyacrylamide hybrid hydrogel via self-assembly of G-quadruplexes (Fig. 11a). That system included just one type of acrydite-modified,

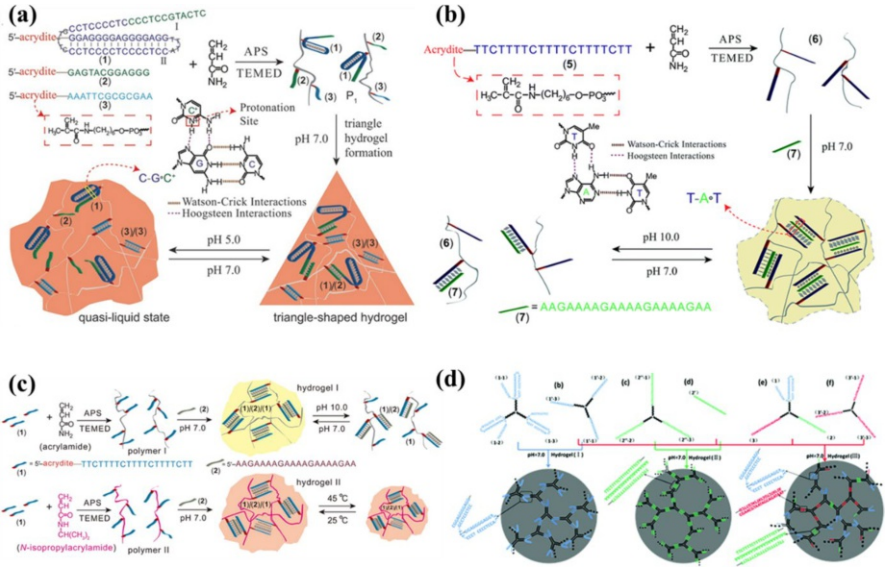

Fig. 10 DNA hydrogel formation using a DNA triplex. **a** Schematic of a pH-responsive hydrogel based on C–G·C $^+$ triplex crosslinking. **b** Synthesis of a DNA hydrogel with T–A·T triplex bridging. **c** Schematic of a DNA–pNIPAM hybrid hydrogel with T–A·T crosslinking. **d** Schematic of a pH-activated DNA triplex for the preparation of a Y-shaped pure DNA hydrogel. Reproduced with permission from [90, 91, 93, 94]

G-containing oligonucleotide. Copolymerization of the acrydite-modified, G-containing oligonucleotide with acrylamide monomer resulted in G-containing copolymer chains. Upon the addition of K^+, the G-containing oligonucleotides on the polyacrylamide chains self-assembled to form interchain G-quadruplexes that crosslinked the copolymer chains, thus inducing the formation of a hydrogel. Given that the crosslinking of the hydrogel depended on the presence of G-quadruplexes, when 18-crown-6 (a K^+ ion chelator) was added to the system, the hydrogel dissociated because the 18-crown-6 abstracted K^+ ions from the G-quadruplexes, causing them to fall apart. Furthermore, G-quadruplexes exhibit HRP-mimicking catalytic activity when they bind to hemin. The authors therefore found that adding hemin to the G-quadruplex-crosslinked acrylamide hydrogel resulted in a system with HRP-mimicking catalytic activity, and that this catalytic activity could be regulated through the addition of K^+ ions or 18-crown-6 [95]. Utilizing the HRP-mimicking catalytic activity of this hydrogel, Willner was able to synthesize polyaniline (Fig. 11b), which was deposited on the hybrid hydrogel, increasing its conductivity [96]. G-quadruplexes were also used as crosslinkers in a DNA hybrid hydrogel with controllable network density (Fig. 11c). The strength of the hydrogel was decreased and its volume was therefore increased by deconstructing the G-quadruplex-based crosslinking; conversely, the strength of the hydrogel was increased and its volume was decreased by enhancing the G-quadruplex-based crosslinking (note that G-quadruplexes were not the only crosslinkers present in the hydrogel, so destroying the G-quadruplexes did not

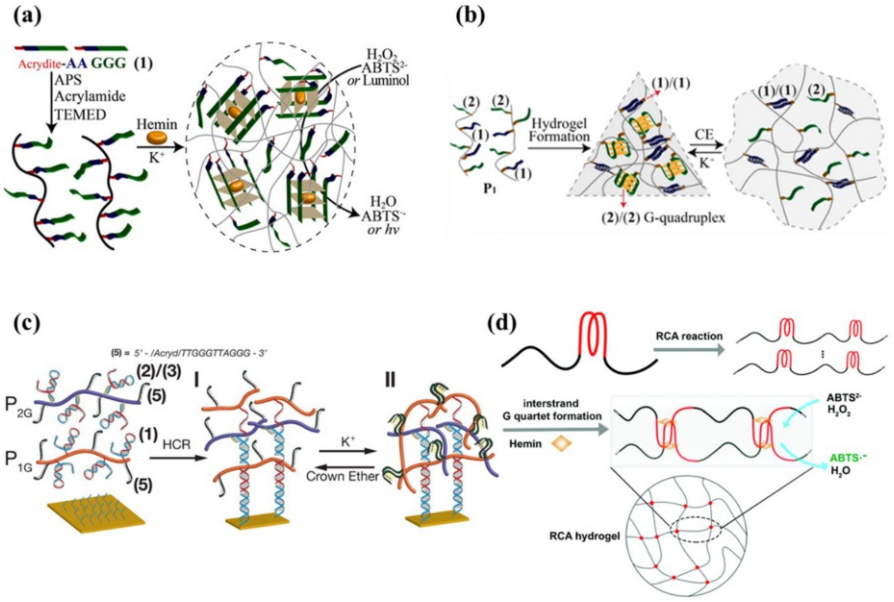

Fig. 11 DNA hydrogels based on G-quadruplexes. **a** Schematic of DNA hydrogel formation based on K^+-stabilized G-quadruplex self-assembly. **b** Schematic of a shape-memory hydrogel with duplex/G-quadruplex double crosslinking. **c** Schematic of the construction of a G-quadruplex-based hydrogel with controllable network density on a gold-plated glass surface. **d** Schematic of the self-assembly of RCA products to form a hydrogel through G-quadruplex generation. Reproduced with permission from [28, 95, 97, 99]

cause the hydrogel to dissociate). Willner's research group has performed a series of studies based on this concept [28, 97, 98].

In another scheme, multi-repeat G-rich sequences were amplified from circular cytosine-rich DNA templates. Rational design of the template sequences permitted the generation of RCA products with the potential to form intermolecular G-quadruplexes under appropriate conditions, which in turn induced the formation of a hydrogel (Fig. 11d). When combined with hemin, this hydrogel presented HRP-like catalytic properties that could be applied in colorimetric bioanalysis [99, 100].

4.3 DNA Hydrogels Based on Metallo Base Pairs

Metallo base pairs such as C–Ag^+–C and T–Hg^{2+}–T can also be used to crosslink and therefore stabilize duplex DNA cooperatively, implying that they can be used to form DNA hydrogels [13]. In 2014, Willner used C–Ag^+–C metallo base pairs to generate a hydrogel for the first time. Y-shaped DNA building blocks and DNA-functionalized acrylamide chains were crosslinked by C–Ag^+–C metallo base pairs to prepare a pure DNA hydrogel and a DNA–polyacrylamide hybrid hydrogel, respectively (Fig. 12a, b). The authors designed a self-complementary DNA sequence with two C–C mismatches, meaning that duplexes were unstable at room

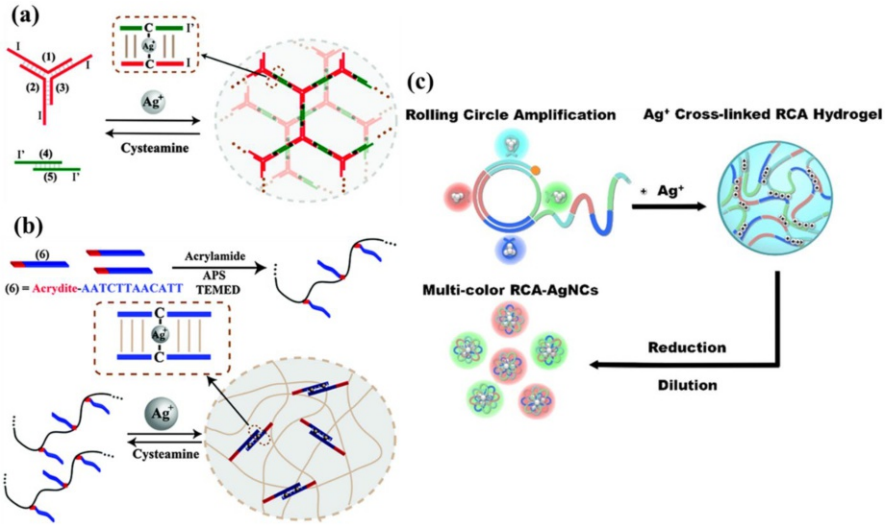

Fig. 12 DNA hydrogel formation based on cytosine–Ag^+–cytosine bridges. **a** Schematic of the Ag^+-induced crosslinking of Y-shaped DNA to form a hydrogel. **b** Schematic of the Ag^+-stimulated formation of a DNA–polyacrylamide hybrid hydrogel. **c** Schematic of the preparation of a hydrogel through the Ag^+-induced crosslinking of RCA products. Reproduced with permission from [101, 103]

temperature and failed to self-assemble into a hydrogel. However, when Ag^+ ions were added to the system, C–Ag^+–C bridges were formed, stabilizing the duplexes and leading to the formation of a hydrogel in which the duplexes acted as crosslinkers [101]. A DNA–pNIPAM hybrid hydrogel was also obtained through the addition of Ag^+ ions [84]. This concept of a hydrogel that is cooperatively crosslinked using Ag^+ ions was also utilized to create a shape-memory hydrogel [102]. Just as above, RCA products with cytosine-rich sequences were produced, and then a DNA hydrogel containing silver nanoclusters was realized through DNA self-assembly based on C–Ag^+–C interactions (Fig. 12c) [103]. Yang reported a different DNA hydrogel with silver nanoclusters that was generated through the physical entanglement of RCA products [104].

5 DNA Hydrogels Formed Using Novel Methods

5.1 Application of Aptamers and DNAzymes as DNA Crosslinkers

As well as the DNA hydrogels generated through traditional DNA interactions described above, a number of new concepts for DNA hydrogel formation have been reported recently. Interestingly, DNA aptamers and DNAzymes have been widely used in these schemes.

Aptamers are single-stranded oligonucleotides that can bind specifically to a target, enabling them to selectively recognize a variety of molecules ranging from macromolecules to small compounds [105]. Using DNA aptamers as crosslinkers

in hydrogels allows the creation of hydrogels that respond to a wide variety of targets. In the absence of the target, the aptamer acts just like a conventional DNA crosslinker, but when the target is present, the aptamer preferentially forms a complex with it, altering the structure of the hydrogel. Based on this principle, a series of hydrogels that respond to particular target molecules have been prepared for use in detection schemes.

In 2008, Tan reported an adenosine-responsive DNA–polyacrylamide hybrid hydrogel with a response mechanism based on aptamer–target interactions. This system was the first reported example of a DNA–polyacrylamide hybrid hydrogel that transitions from gel to solution upon the addition of adenosine (Fig. 13a). The method used to prepare the hydrogel was similar to that employed by Lin [19]. First, two acrydite-modified oligonucleotides named strand A and strand B were separately copolymerized with acrylamide, leading to two types of DNA-grafted polyacrylamide chains. These two DNA-grafted polyacrylamide chains were then mixed in solution at stoichiometric concentrations. Finally, the adenosine-responsive DNA–polyacrylamide hybrid hydrogel was generated by the addition of the linker DNA, which had an aptamer sequence for adenosine at the 3′ end. Thus, when adenosine was added to the hydrogel, the aptamer sequence of the DNA linker formed a complex with the adenosine, leading to the dissociation of strand B from the linker. This triggered the dissociation of the crosslinking network in the

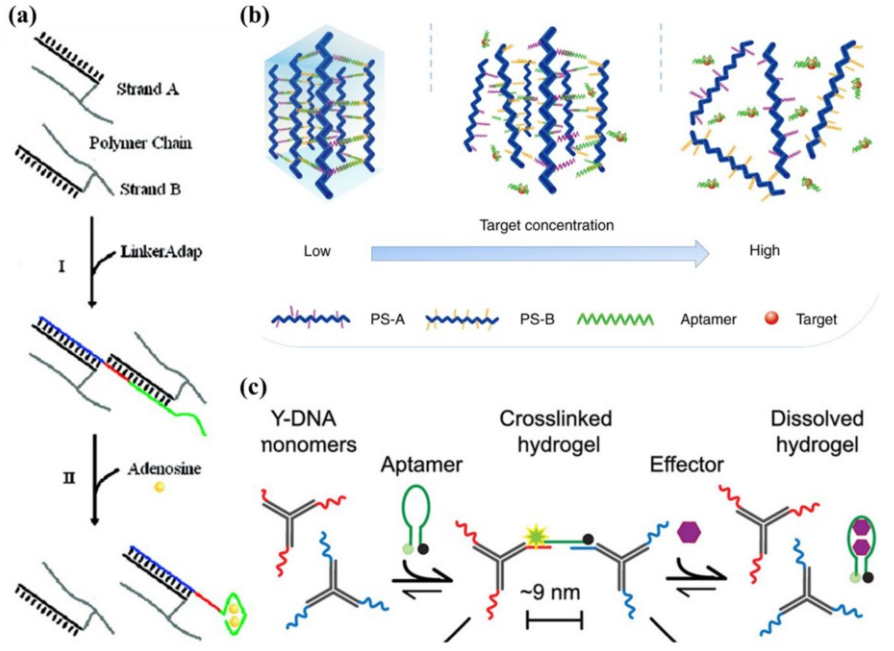

Fig. 13 Use of aptamers as crosslinkers in DNA hydrogel formation. **a** Schematic of an adenosine-responsive DNA hydrogel. **b** Schematic showing that the degree of hydrogel degradation was positively correlated with the concentration of the target. **c** Schematic of an adenosine-responsive DNA hydrogel based on the Y-DNA hydrogel model. Reproduced with permission from [106, 119, 123]

hydrogel; in other words, the hydrogel collapsed. A detection technique based on this concept of adenosine-induced hydrogel dissociation was also developed. First, gold nanoparticles used as indicators were mixed with solutions of the two DNA-grafted polyacrylamide chains before gelation. Upon adding the linker to form a hydrogel, gold nanoparticles were trapped in the hydrogel network. When adenosine was added, the hydrogel network collapsed and the gold nanoparticles were released into the solution, yielding obvious visual signals [106]. Since that report was published, aptamer-responsive hydrogels have been widely used for various biomedical applications, including sensing, diagnostics, and drug loading [107], and DNA linkers with aptamers for cocaine [108], ATP [109], AS1411 [107], ochratoxin A [110], aflatoxin B1 [111], and thrombin [112] (among others) have been developed for use in aptamer-responsive DNA hydrogels. In the context of applying aptamer-responsive hydrogels to biological detection and analysis, Yang's research group has constructed a series of detection devices and equipment based on this principle [110, 111, 113–119]. For example, a personal glucose meter that can be used to determine the concentrations of targets other than glucose was developed [113]. A volumetric bar-chart chip (V-Chip) device containing a target-responsive hydrogel was also devised as a means to detect specific targets [114]. Moreover, making use of the thermoreversible nature of DNA hydrogels and the principle of capillary action, a target-responsive hydrogel film in a capillary tube was created that permitted the quantitative detection of the target. It is worth mentioning that this sensor did not rely on hydrogel dissociation to detect the target: only a slight change in the internal structure of the hydrogel was required to quantitatively detect the concentration of the target in sample solutions. The only equipment required was a capillary tube (Fig. 13b) [119].

In contrast to using only one type of aptamer as the linker to construct an aptamer-responsive hydrogel, Tan and coworkers developed dual-responsive hydrogels that incorporated both ATP and cocaine aptamers, and then creating a logic gate system based on thse dual-responsive hydrogels. The authors realized AND and OR logic gates by constructing two dual-aptamer linkers with different structures. For the AND gate, a DNA linker with a cocaine aptamer sequence was mixed with two types of DNA-grafted polyacrylamide chains, one of which contained an ATP aptamer sequence. These three kinds of single-stranded DNAs assembled into a hydrogel consisting of Y-shaped crosslinker units. The hydrogel was only dissociated when both ATP and cocaine were added because only then were the Y-shaped crosslinker units completely disintegrated. For the OR gate, the DNA linker contained both cocaine and ATP aptamer sequences located at opposite ends of the DNA strand. This DNA linker was added to DNA-grafted polyacrylamide chains to produce a hydrogel in which the DNA linker was the only component that was responsive to either ATP or cocaine; upon the addition of either ATP or cocaine to the hydrogel, the crosslinked network was destroyed and the hydrogel collapsed [120].

Aptamers can also be used as crosslinkers in pure DNA hydrogels. Lei and coworkers reported a pure DNA hydrogel that was constructed using a Y-shaped DNA and a thrombin aptamer linker through DNA self-assembly. Au nanoparticles (AuNPs) trapped in the hydrogel network were used as a signal indicator.

Upon adding thrombin, a complex of L-DNA aptamer with thrombin was generated, inducing the collapse and dissolution of the DNA hydrogel. This released the AuNPs, leading to a change in the color of the upper solution [121]. An aptamer for ochratoxin A was used as a DNA linker to construct a pure DNA hydrogel that was sensitive to ochratoxin A [122]. An adenine-responsive hydrogel was designed for use as a quantitative tool to measure the responsiveness and dissolution kinetics of this type of hydrogel (Fig. 13c) [123, 124]. Integrating an ATP aptamer into the DNA linker of a hydrogel also allowed the mechanical properties of the hydrogel to be tuned [125].

Other hydrogels that incorporate an aptamer do not use the aptamer as a crosslinker. For example, Chai and Yuan constructed a DNA hydrogel using a strategy similar to that employed for the second type of hydrogel (type II) created by Nagahara and Matsuda [15]. Three acrydite-modified DNA strands named S1, S2, and S3 were used, where S1 and S2 were complementary to each other. Two kinds of DNA-grafted polyacrylamide chains named P1 and P2 were employed; P1 was obtained by copolymerizing S1 with S3 and acrylamide monomer while P2 was obtained by copolymerizing S2 with S3 and acrylamide monomer. The DNA fragment on S1 in P1 was hybridized with a heparanase aptamer (HPA), which blocked hybridization with DNA fragments on S2 in P2. As a result, no hydrogel formation was possible until the addition of HPA. When HPA was added, the aptamer of HPA dissociated from P1, forming a HPA–aptamer complex. This meant that the DNA fragment on S1 could hybridize with the DNA fragment on S2, leading to crosslinking between P1 and P2 and the formation of a hydrogel. Based on this strategy, the authors developed a sensor for use in a heparinase (HPA) bioassay [126]. In addition, Du created a DNA hydrogel through the one-pot self-assembly of X-shaped DNA, a DNA linker, and an aptamer, but in this case the aptamer was only used as a functional unit for target protein capture, not to change the hydrogel network in the presence of the target [127]. Tan developed a DNA nanohydrogel that was efficiently taken up by cells due to the recognition of an aptamer in the nanohydrogel by the target cells. Although the nanohydrogel was eventually destroyed, this was induced not by the aptamer but by the disruption of disulfide linkages in the DNA strands [128].

DNAzymes can also be used as DNA crosslinkers. A DNAzyme is a single-stranded DNA that has a special sequence and secondary structure and presents a level of catalytic activity similar to that of normal enzymes [129, 130]. One DNAzyme is metal ion dependent; in the presence of certain metal ions, its ability to cleave nucleic acid molecules is activated, and the activated DNAzyme then irreversibly cleaves substrate nucleic acid molecules at the cleavage site [131]. This type of DNAzyme could be used in a DNA crosslinker to construct DNA hydrogels that are responsive to particular target metal ions.

In 2011, Yang provided the first report of a Cu^{2+}-responsive DNAzyme-crosslinked DNA–polyacrylamide hybrid hydrogel. To obtain this hydrogel, two kinds of single-stranded DNAs, DNAzyme, and substrate were incorporated into linear polyacrylamide, which yielded two kinds of DNA-grafted polyacrylamide chains, DNAzyme-grafted polyacrylamide chains, and substrate-grafted polyacrylamide chains. When the two kinds of DNA-grafted polyacrylamide chains were

mixed, the DNAzyme and the substrate on the polyacrylamide chains combined to form a DNAzyme–substrate complex, thus crosslinking the polyacrylamide chains and forming a hydrogel. The DNAzyme–substrate complex contained a domain that specifically recognized Cu^{2+}. When Cu^{2+} was added, the DNAzyme–substrate complex dissociated. Because the substrate was irreversibly cleaved by the DNAzyme, the hydrogel eventually dissolved. AuNPs were also introduced into the hydrogel as a colorimetric indicator in order to develop a Cu^{2+} sensor (Fig. 14a) [132]. Based on this strategy, various metal-ion-dependent DNAzymes have been used in the DNA crosslinkers of metal-ion-responsive hydrogels, including those that are sensitive to Pb^{2+} (Fig. 14b) [133, 134], UO^{2+} (Fig. 14c) [135], Mg^{2+} (Fig. 14d) [136], Zn^{2+} (Fig. 14d) [136], among others.

5.2 Control of DNA Hydrogel Formation Using Light

Light-responsive DNA has also been used to form gel networks. It is well known that the hybridization of DNA strands can be controlled by light. The most common strategy that utilizes this phenomenon involves the integration of azobenzene into single-stranded DNA. In 2011, Tan and colleagues integrated azobenzene into single-stranded DNA and used the resulting DNA as a crosslinker to

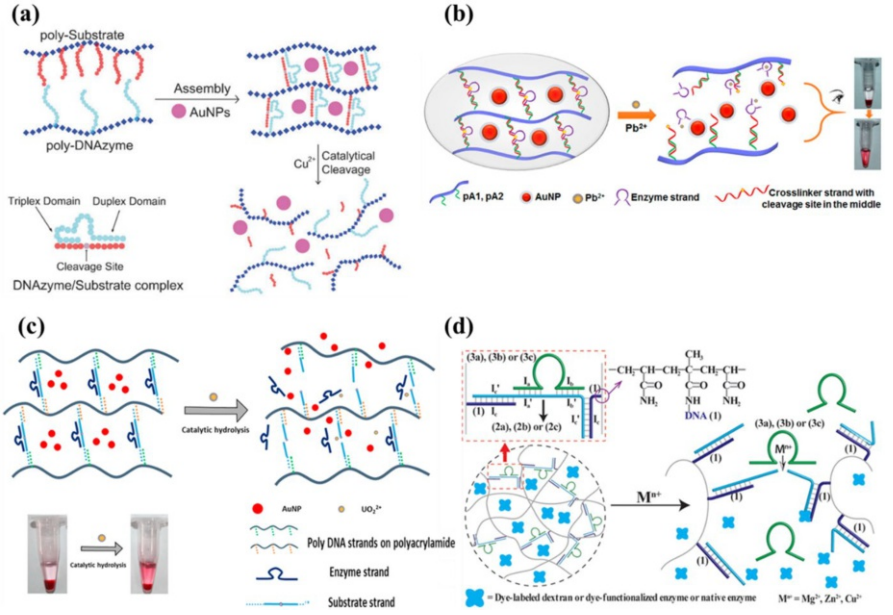

Fig. 14 DNAzymes used as crosslinkers in DNA hydrogel formation. **a** Schematic of a hydrogel which uses a DNAzyme crosslinker that is responsive to copper ion. **b** Schematic of a hydrogel which uses a DNAzyme crosslinker that is responsive to lead ion and is employed for visual detection. **c** Schematic of a hydrogel which uses a DNAzyme crosslinker that is responsive to uranyl ion and is employed in sensors. **d** Schematic of a detection platform based on the use of metal-ion-dependent DNAzyme/substrate sequences as crosslinkers. Reproduced with permission from [132, 133, 135, 136]

form a photoresponsive DNA hybrid hydrogel. This hydrogel exhibited reversible hydrogel to solution phase transitions that were controllable using light (Fig. 15a) due to the *trans*/*cis* photoisomerization of azobenzene, as the hybridization of the DNA linker with its complementary strand was dependent on the isomer of azobenzene present. Irradiation with 450-nm light led to *trans*-azobenzene, meaning that the linker DNA could hybridize with its complementary strand tethered to the polyacrylamide polymer chains, thus inducing hydrogel formation.

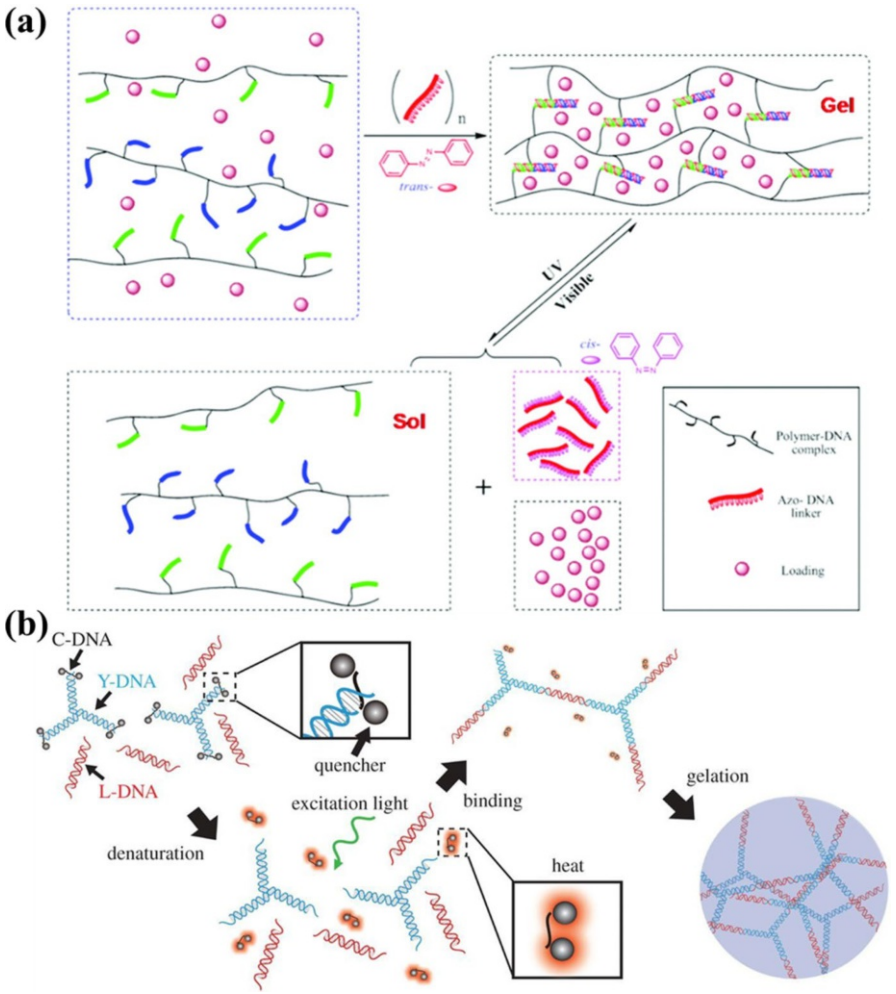

Fig. 15 Schematic of light-controllable DNA hydrogel formation. **a** Azo-incorporated DNA is used as a crosslinker to form the hydrogel, which enables the crosslinking process to be reversibly controlled by visible and UV light. **b** Schematic of photothermally induced DNA hydrogel formation. In this concept, thermal energy causes the Y-DNA to dissociate from the C-DNA and then link with L-DNA to create the DNA hydrogel. Reproduced with permission from [137, 138]

Irradiation with 350-nm light resulted in *cis*-azobenzene, which did not permit hybridization and caused the hydrogel to dissociate [137].

Light-controllable DNA hydrogels can also be achieved indirectly, using a photothermal approach. In 2018, Tanida and coworkers realized light-controllable DNA hydrogel formation based on a Y-scaffold and linker system. In this scheme, a ssDNA denoted Cap-DNA (C-DNA) was used that had quenchers at both ends and was complementary to the sticky ends of Y-DNA, meaning that the C-DNA prevented L-DNA from linking to the Y-DNA. Upon excitation with light, the quenchers became heat sources and the thermal energy they emitted caused the Y-DNA to dissociate from the C-DNA and link with the L-DNA, resulting in the creation of a DNA hydrogel (Fig. 15b). Furthermore, the shape of the hydrogel could be tailored by adjusting the irradiation pattern [138].

5.3 DNA Hydrogel Formation Based on Clamped HCR

Another novel mechanism that can be used to form gel networks is clamped HCR (C-HCR). Hybridization chain reaction (HCR), a type of toehold-mediated strand displacement (TMSD) reaction, was first developed and named by Dirks and Pierce in 2004 [139], and it has since attracted great interest due to its enzyme-free nature, isothermal conditions, simple protocols, and admirable amplification efficiency. In a typical linear HCR, a short ssDNA initiates the cross-opening of two DNA hairpins, yielding nicked double-helix DNA polymers [140]. Although there was a report of the use of HCR to form gel networks in 2015 [28], it was not used to prepare pure DNA hydrogels until clamped HCR was designed by Liu and coworkers [141]. Using clamped HCR, those authors prepared a 3D DNA hydrogel with favorable spatial and temporal control.

The process used to construct the DNA hydrogel using clamped HCR was as follows (Fig. 16a). Two kinds of hairpin strands were used, one of which (H1) was specifically designed for use in a clamped HCR system as it had palindromic sequences

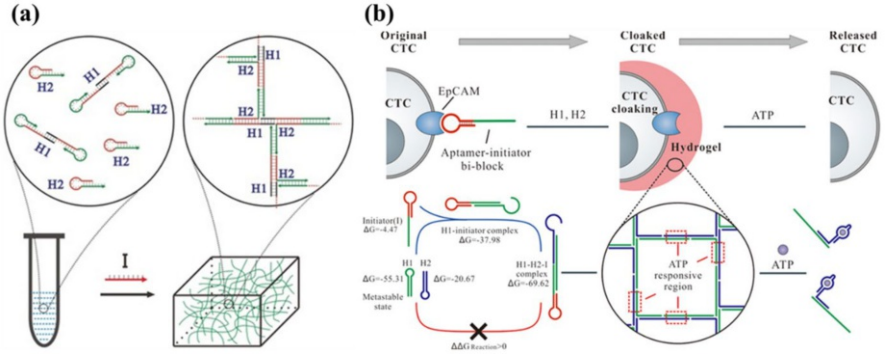

Fig. 16 Schematic of hydrogel formation based on clamped HCR. **a** Schematic of the utilization of clamped HCR for DNA hydrogel formation. **b** Schematic of an ATP-responsive DNA hydrogel cloaked on a cell surface; the aptamer-triggered hydrogel was obtained using clamped HCR. Reproduced with permission from [141, 142]

at its 5′ end. The other hairpin strand was denoted H2. After annealing, an H1 dimer was formed due to hybridization of the palindromic sequences of H1. This H1 dimer and H2 coexisted in a metastable state until a small amount of initiator was added to the system. The introduction of the initiator triggered immediate HCR, which yielded HCR products. The H1 dimer had two branches, so it could form a three-arm junction (with one initiator and one H2 strand) or a four-arm junction (with two H2 strands) in divergent chain reactions during the C-HCR. The products of the clamped HCR were then crosslinked to form a DNA hydrogel [141].

Using a similar strategy, a method permitting the in situ formation of a DNA hydrogel on the surfaces of circulating tumor cells (CTCs) was developed (Fig. 16b). The authors first designed a specific aptamer initiator that specifically recognized epithelial cell adhesion molecule (EpCAM) on the CTC surface, as this specific aptamer initiator could then be anchored to the CTC surface. When the H1 dimer and H2 encountered the initiator on the CTC surface, a DNA hydrogel was formed via clamped HCR. An ATP aptamer was also incorporated into H2, causing the dissociation of the hydrogel in the presence of ATP and thus a phase transition from hydrogel to solution. The authors described the overall process as an aptamer-trigger clamped hybridization chain reaction (atcHCR) [142].

6 Conclusion and Outlook

In summary, DNA self-assembly has been found to be an effective approach to hydrogel creation. In this review, we divided DNA hydrogels into four categories according to the gelation mechanism: DNA hydrogels formed by conventional DNA hybridization, DNA hydrogels formed with the assistance of enzymes, DNA hydrogels based on the use of special DNA structures, and DNA hydrogels formed using novel methods. Various synthetic strategies and applications of DNA hydrogels have been detailed.

It is worth noting that among these hydrogels, stimuli-responsive and biologically compatible DNA hybrid hydrogels have received extensive attention [143]. A wide range of tailored DNAs can potentially be used as crosslinkers to achieve stimuli responsiveness, e.g., a DNA “toehold” can be used to achieve sensitivity to nucleic acid molecules [19], aptamers can be applied to enhance the response to the target [106], DNAzymes can be used to improve the response to metal ions [132], and azobenzene-modified DNA can be employed to achieve light sensitivity [137]. Since these hydrogels have specific stimuli-responsive behaviors, they have been widely used as biosensors in the field of bioanalysis [144, 145]. In addition, pure DNA hydrogels have excellent biocompatibilities and biodegradabilities, which makes them superior carriers for drug delivery [146].

Due to the high cost of DNA, the large-scale use of DNA hybrid hydrogels and pure DNA hydrogels has been limited [147]. Although the amount of DNA used in DNA hybrid hydrogels is relatively small, it is usually necessary to chemically modify the DNA used [148–151], and the price of chemically modified DNA is very expensive [146, 147, 152–154]. Therefore, it is particularly important to develop

efficient and inexpensive DNA synthesis and modification methods to overcome this obstacle [155–158].

Moreover, nano/micro-DNA hydrogels may be an important research direction in the future, especially in the field of intracellular drug delivery, since nano/micro-DNA hydrogels have the advantages that they passively target tumor cells and they rapidly respond to stimuli [4].

Finally, the clamped HCR strategy that is sometimes used to construct DNA hydrogels permits high spatial and temporal control. It is worth mentioning that hydrogels are formed under physiological conditions using this method, and only a small amount of the initiator DNA is required. Hydrogels obtained through the rational design of DNA sequences could have specific biological functions [141, 142].

Acknowledgements The authors acknowledge financial support by the National Natural Science Foundation of China (21722310), the Youth Innovation Promotion Association of CAS (2012205, 2016236), the Fundamental Research Funds for the Central Universities, and the LU JIAXI International team program supported by the K.C. Wong Education Foundation and CAS.

Compliance with Ethical Standards

Conflict of interest On behalf of all the authors, the corresponding author states that there is no conflict of interest.

References

1. Peppas NA, Bures P, Leobandung W, Ichikawa H (2000) Eur J Pharm Biopharm 50:27. https://doi.org/10.1016/s0939-6411(00)00090-4
2. Drury JL, Mooney DJ (2003) Biomaterials 24:4337. https://doi.org/10.1016/s0142-9612(03)00340-5
3. Gawel K, Barriet D, Sletmoen M, Stokke BT (2010) Sensors 10:4381. https://doi.org/10.3390/s100504381
4. Li J, Mooney DJ (2016) Nat Rev Mater 1:16071. https://doi.org/10.1038/natrevmats.2016.71
5. Peppas NA, Hilt JZ, Khademhosseini A, Langer R (2006) Adv Mater 18:1345. https://doi.org/10.1002/adma.200501612
6. Watson JD, Crick FH (1974) Nature 248:765. https://doi.org/10.1038/248765a0
7. Seeman NC (1982) J Theor Biol 99:237. https://doi.org/10.1016/0022-5193(82)90002-9
8. Seeman NC (1998) Annu Rev Biophys Biomol Struct 27:225. https://doi.org/10.1146/annurev.biophys.27.1.225
9. Seeman NC (2003) Nature 421:427. https://doi.org/10.1038/nature01406
10. Wang ZG, Ding B (2013) Adv Mater 25:3905. https://doi.org/10.1002/adma.201301450
11. Jones MR, Seeman NC, Mirkin CA (2015) Science 347:1260901. https://doi.org/10.1126/science.1260901
12. Li F, Tang J, Geng J, Luo D, Yang D (2019) Prog Polym Sci 98:101163. https://doi.org/10.1016/j.progpolymsci.2019.101163
13. Kahn JS, Hu Y, Willner I (2017) Acc Chem Res 50:680. https://doi.org/10.1021/acs.accounts.6b00542
14. Amiya T, Tanaka T (1987) Macromolecules 20:1162. https://doi.org/10.1021/ma00171a050
15. Nagahara S, Matsuda T (1996) Polym Gels Netw 4:111. https://doi.org/10.1016/0966-7822(96)00001-9
16. Um SH, Lee JB, Park N, Kwon SY, Umbach CC, Luo D (2006) Nat Mater 5:797. https://doi.org/10.1038/nmat1741

17. Cheng E, Xing Y, Chen P, Yang Y, Sun Y, Zhou D, Xu L, Fan Q, Liu D (2009) Angew Chem Int Ed Engl 48:7660. https://doi.org/10.1002/anie.200902538
18. Xing Y, Cheng E, Yang Y, Chen P, Zhang T, Sun Y, Yang Z, Liu D (2011) Adv Mater 23:1117. https://doi.org/10.1002/adma.201003343
19. Lin DC, Yurke B, Langrana NA (2004) J Biomech Eng Trans ASME 126:104. https://doi.org/10.1115/1.1645529
20. Lin DC, Yurke B, Langrana NA (2005) J Mater Res 20:1456. https://doi.org/10.1557/jmr.2005.0186
21. Liedl T, Dietz H, Yurke B, Simmel F (2007) Small 3:1688. https://doi.org/10.1002/smll.200700366
22. He Y, Yang X, Yuan R, Chai Y (2017) Anal Chem 89:8538. https://doi.org/10.1021/acs.analchem.7b02321
23. Liu S, Su W, Li Y, Zhang L, Ding X (2018) Biosens Bioelectron 103:1. https://doi.org/10.1016/j.bios.2017.12.021
24. Si Y, Li L, Wang N, Zheng J, Yang R, Li J (2019) ACS Appl Mater Interfaces 11:7792. https://doi.org/10.1021/acsami.8b21727
25. Cai W, Xie S, Zhang J, Tang D, Tang Y (2017) Biosens Bioelectron 98:466. https://doi.org/10.1016/j.bios.2017.07.025
26. Li C, Li H, Ge J, Jie G (2019) Chem Commun 55:3919. https://doi.org/10.1039/c9cc00565j
27. Lyu D, Chen S, Guo W (2018) Small 14:1704039. https://doi.org/10.1002/smll.201704039
28. Kahn JS, Trifonov A, Cecconello A, Guo W, Fan C, Willner I (2015) Nano Lett 15:7773. https://doi.org/10.1021/acs.nanolett.5b04101
29. Cangialosi A, Yoon C, Liu J, Huang Q, Guo J, Nguyen TD, Gracias DH, Schulman R (2017) Science 357:1126. https://doi.org/10.1126/science.aan3925
30. Fern J, Schulman R (2018) Nat Commun 9:3766. https://doi.org/10.1038/s41467-018-06218-w
31. English MA, Soenksen LR, Gayet RV, de Puig H, Angenent-Mari NM, Mao AS, Nguyen PQ, Collins JJ (2019) Science 365:780. https://doi.org/10.1126/science.aaw5122
32. Han D, Li J, Tan W (2019) Science 365:754. https://doi.org/10.1126/science.aay4198
33. Jin J, Xing Y, Xi Y, Liu X, Zhou T, Ma X, Yang Z, Wang S, Liu D (2013) Adv Mater 25:4714. https://doi.org/10.1002/adma.201301175
34. Chen P, Li C, Liu D, Li Z (2012) Macromolecules 45:9579. https://doi.org/10.1021/ma302233m
35. Li C, Faulkner-Jones A, Dun AR, Jin J, Chen P, Xing Y, Yang Z, Li Z, Shu W, Liu D, Duncan RR (2015) Angew Chem Int Ed Engl 54:3957. https://doi.org/10.1002/anie.201411383
36. Li C, Rowland MJ, Shao Y, Cao T, Chen C, Jia H, Zhou X, Yang Z, Scherman OA, Liu D (2015) Adv Mater 27:3298. https://doi.org/10.1002/adma.201501102
37. Zhou X, Li C, Shao Y, Chen C, Yang Z, Liu D (2016) Chem Commun 52:10668. https://doi.org/10.1039/c6cc04724f
38. Ma X, Yang Z, Wang Y, Zhang G, Shao Y, Jia H, Cao T, Wang R, Liu D (2017) ACS Appl Mater Interfaces 9:1995. https://doi.org/10.1021/acsami.6b12327
39. Wang Y, Shao Y, Ma X, Zhou B, Faulkner-Jones A, Shu W, Liu D (2017) ACS Appl Mater Interfaces 9:12311. https://doi.org/10.1021/acsami.7b01604
40. Li C, Zhou X, Shao Y, Chen P, Xing Y, Yang Z, Li Z, Liu D (2017) Mater Chem Front 1:654. https://doi.org/10.1039/C6QM00176A
41. Xing Z, Caciagli A, Cao T, Stoev I, Zupkauskas M, O'Neill T, Wenzel T, Lamboll R, Liu D, Eiser E (2018) Proc Natl Acad Sci 115:8137. https://doi.org/10.1073/pnas.1722206115
42. Li C, Chen P, Shao Y, Zhou X, Wu Y, Yang Z, Li Z, Weil T, Liu D (2015) Small 11:1138. https://doi.org/10.1002/smll.201401906
43. Gacanin J, Kovtun A, Fischer S, Schwager V, Quambusch J, Kuan SL, Liu W, Boldt F, Li C, Yang Z, Liu D, Wu Y, Weil T, Barth H, Ignatius A (2017) Adv Healthc Mater 6:1700392. https://doi.org/10.1002/adhm.201700392
44. Guo W, Orbach R, Mironi-Harpaz I, Seliktar D, Willner I (2013) Small 9:3748. https://doi.org/10.1002/smll.201300055
45. Van Nguyen K, Minteer SD (2015) Chem Commun (Camb) 51:13071. https://doi.org/10.1039/c5cc04810a
46. Van Khiem N, Holade Y, Minteer SD (2016) Acs Catalysis 6:2603. https://doi.org/10.1021/acscatal.5b02699
47. Shao Y, Sun Z-Y, Wang Y, Zhang B-D, Liu D, Li Y-M (2018) ACS Appl Mater Interfaces 10:9310. https://doi.org/10.1021/acsami.8b00312

48. Ren N, Sun R, Xia K, Zhang Q, Li W, Wang F, Zhang X, Ge Z, Wang L, Fan C, Zhu Y (2019) ACS Appl Mater Interfaces 11:26704. https://doi.org/10.1021/acsami.9b08652
49. Nishikawa M, Ogawa K, Umeki Y, Mohri K, Kawasaki Y, Watanabe H, Takahashi N, Kusuki E, Takahashi R, Takahashi Y, Takakura Y (2014) J Control Release 180:25. https://doi.org/10.1016/j.jconrel.2014.02.001
50. Nishida Y, Ohtsuki S, Araie Y, Umeki Y, Endo M, Emura T, Hidaka K, Sugiyama H, Takahashi Y, Takakura Y, Nishikawa M (2016) Nanomed Nanotechnol Biol Med 12:123. https://doi.org/10.1016/j.nano.2015.08.004
51. Ishii-Mizuno Y, Umeki Y, Onuki Y, Watanabe H, Takahashi Y, Takakura Y, Nishikawa M (2017) Int J Pharm 516:392. https://doi.org/10.1016/j.ijpharm.2016.11.048
52. Nomura D, Saito M, Takahashi Y, Takahashi Y, Takakura Y, Nishikawa M (2018) Int J Pharm 547:556. https://doi.org/10.1016/j.ijpharm.2018.06.029
53. Umeki Y, Saito M, Takahashi Y, Takakura Y, Nishikawa M (2017) Adv Healthc Mater 6:1700355. https://doi.org/10.1002/adhm.201700355
54. Yata T, Takahashi Y, Tan M, Nakatsuji H, Ohtsuki S, Murakami T, Imahori H, Umeki Y, Shiomi T, Takakura Y, Nishikawa M (2017) Biomaterials 146:136. https://doi.org/10.1016/j.biomaterials.2017.09.014
55. Bomboi F, Romano F, Leo M, Fernandez-Castanon J, Cerbino R, Bellini T, Bordi F, Filetici P, Sciortino F (2016) Nat Commun 7:13191. https://doi.org/10.1038/ncomms13191
56. Fernandez-Castanon J, Bianchi S, Saglimbeni F, Di Leonardo R, Sciortino F (2018) Soft Matter 14:6431. https://doi.org/10.1039/c8sm00751a
57. Nguyen DT, Saleh OA (2017) Soft Matter 13:5421. https://doi.org/10.1039/c7sm00557a
58. Zhang L, Jean SR, Ahmed S, Aldridge PM, Li X, Fan F, Sargent EH, Kelley SO (2017) Nat Commun 8:381. https://doi.org/10.1038/s41467-017-00298-w
59. Meng X, Zhang K, Dai W, Cao Y, Yang F, Dong H, Zhang X (2018) Chem Sci 9:7419. https://doi.org/10.1039/c8sc02858c
60. Guo B, Wen B, Cheng W, Zhou X, Duan X, Zhao M, Xia Q, Ding S (2018) Biosens Bioelectron 112:120. https://doi.org/10.1016/j.bios.2018.04.027
61. Noll T, Schonherr H, Wesner D, Schopferer M, Paululat T, Noll G (2014) Angew Chem Int Ed Engl 53:8328. https://doi.org/10.1002/anie.201402497
62. Noll T, Wenderhold-Reeb S, Bourdeaux F, Paululat T, Noll G (2018) Chemistryselect 3:10287. https://doi.org/10.1002/slct.201802364
63. Pan W, Wen H, Niu L, Su C, Liu C, Zhao J, Mao C, Liang D (2016) Soft Matter 12:5537. https://doi.org/10.1039/c6sm00283h
64. Oishi M, Nakatani K (2019) Small 15:1900490. https://doi.org/10.1002/smll.201900490
65. Jiang H, Pan V, Vivek S, Weeks ER, Ke Y (2016) ChemBioChem 17:1156. https://doi.org/10.1002/cbic.201500686
66. Park N, Kahn JS, Rice EJ, Hartman MR, Funabashi H, Xu J, Um SH, Luo D (2009) Nat Protoc 4:1759. https://doi.org/10.1038/nprot.2009.174
67. Ruiz RCH, Kiatwuthinon P, Kahn JS, Roh YH, Luo D (2012) Ind Biotechnol 8:372. https://doi.org/10.1089/ind.2012.0024
68. Shin SW, Park KS, Shin WJ, Um SH (2015) Small 11:5515. https://doi.org/10.1002/smll.201501334
69. Song J, Lee M, Kim T, Na J, Jung Y, Jung GY, Kim S, Park N (2018) Nat Commun 9:4331. https://doi.org/10.1038/s41467-018-06864-0
70. Nishikawa M, Mizuno Y, Mohri K, Matsuoka N, Rattanakiat S, Takahashi Y, Funabashi H, Luo D, Takakura Y (2011) Biomaterials 32:488. https://doi.org/10.1016/j.biomaterials.2010.09.013
71. Song J, Hwang S, Im K, Hur J, Nam J, Hwang S, Ahn GO, Kim S, Park N (2015) J Mater Chem B 3:1537. https://doi.org/10.1039/c4tb01519c
72. Song J, Im K, Hwang S, Hur J, Nam J, Ahn GO, Hwang S, Kim S, Park N (2015) Nanoscale 7:9433. https://doi.org/10.1039/c5nr00858a
73. Shin SW, Park KS, Jang MS, Song WC, Kim J, Cho S-W, Lee JY, Cho JH, Jung S, Um SH (2015) Langmuir 31:912. https://doi.org/10.1021/la503754e
74. Kim T, Park S, Lee M, Baek S, Lee JB, Park N (2016) Biomicrofluidics 10:034112. https://doi.org/10.1063/1.4953046
75. Hur J, Im K, Hwang S, Choi B, Kim S, Hwang S, Park N, Kim K (2013) Sci Rep 3:1282. https://doi.org/10.1038/srep01282

76. Hur J, Im K, Kim SW, Kim UJ, Lee J, Hwang S, Song J, Kim S, Hwang S, Park N (2013) J Mater Chem A 1:14460. https://doi.org/10.1039/c3ta13382f
77. Noll T, Wenderhold-Reeb S, Schonherr H, Noll G (2017) Angew Chem Int Ed Engl 56:12004. https://doi.org/10.1002/anie.201705001
78. Hartman MR, Yang D, Tran TN, Lee K, Kahn JS, Kiatwuthinon P, Yancey KG, Trotsenko O, Minko S, Luo D (2013) Angew Chem Int Ed Engl 52:8699. https://doi.org/10.1002/anie.201302175
79. Chen T, Romesberg FE (2017) Angew Chem Int Ed Engl 56:14046. https://doi.org/10.1002/anie.201707367
80. Deng S, Yan J, Wang F, Su Y, Zhang X, Li Q, Liu G, Fan C, Pei H, Wan Y (2019) Biosens Bioelectron 137:263. https://doi.org/10.1016/j.bios.2019.04.053
81. Xiang B, He K, Zhu R, Liu Z, Zeng S, Huang Y, Nie Z, Yao S (2016) ACS Appl Mater Interfaces 8:22801. https://doi.org/10.1021/acsami.6b03572
82. Hua X, Zhou X, Guo S, Zheng T, Yuan R, Xu W (2019) Microchim Acta 186:158. https://doi.org/10.1007/s00604-019-3283-2
83. Cheng E, Li Y, Yang Z, Deng Z, Liu D (2011) Chem Commun (Camb) 47:5545. https://doi.org/10.1039/c1cc11028d
84. Guo W, Lu C-H, Qi X-J, Orbach R, Fadeev M, Yang H-H, Willner I (2014) Angew Chem Int Ed Engl 53:10134. https://doi.org/10.1002/anie.201405692
85. Guo W, Lu CH, Orbach R, Wang F, Qi XJ, Cecconello A, Seliktar D, Willner I (2015) Adv Mater 27:73. https://doi.org/10.1002/adma.201403702
86. Wang CY, Li FY, Bi YH, Guo WW (2019) Adv Mater Interfaces 6:1900556. https://doi.org/10.1002/admi.201900556
87. Jia H, Shi J, Shao Y, Liu D (2017) Chin J Polym Sci 35:1307. https://doi.org/10.1007/s10118-017-1978-6
88. Shi J, Jia H, Liu D (2017) Acta Polym Sin 1:135. https://doi.org/10.11777/j.issn1000-3304.2017.16278
89. Xu W, Huang Y, Zhao H, Li P, Liu G, Li J, Zhu C, Tian L (2017) Chemistry 23:18276. https://doi.org/10.1002/chem.201704390
90. Ren J, Hu Y, Lu CH, Guo W, Aleman-Garcia MA, Ricci F, Willner I (2015) Chem Sci 6:4190. https://doi.org/10.1039/c5sc00594a
91. Hu Y, Lu C, Guo W, Aleman-Garcia MA, Ren J, Willner I (2015) Adv Funct Mater 25:6867. https://doi.org/10.1002/adfm.201503134
92. Hu Y, Guo W, Kahn JS, Aleman-Garcia MA, Willner I (2016) Angew Chem Int Ed Engl 55:4210. https://doi.org/10.1002/anie.201511201
93. Hu Y, Kahn JS, Guo W, Huang F, Fadeev M, Harries D, Willner I (2016) J Am Chem Soc 138:16112. https://doi.org/10.1021/jacs.6b10458
94. Lu S, Wang S, Zhao J, Sun J, Yang X (2018) Chem Commun 54:4621. https://doi.org/10.1039/c8cc01603h
95. Lu CH, Qi XJ, Orbach R, Yang HH, Mironi-Harpaz I, Seliktar D, Willner I (2013) Nano Lett 13:1298. https://doi.org/10.1021/nl400078g
96. Lu C, Guo W, Qi X, Neubauer A, Paltiel Y, Willner I (2015) Chem Sci 6:6659. https://doi.org/10.1039/c5sc02203g
97. Lu CH, Guo W, Hu Y, Qi XJ, Willner I (2015) J Am Chem Soc 137:15723. https://doi.org/10.1021/jacs.5b06510
98. Wu Y, Wang D, Willner I, Tian Y, Jiang L (2018) Angew Chem Int Ed Engl 57:7790. https://doi.org/10.1002/anie.201803222
99. Huang Y, Xu W, Liu G, Tian L (2017) Chem Commun 53:3038. https://doi.org/10.1039/c7cc00636e
100. Mao X, Pan S, Zhou D, He X, Zhang Y (2019) Sens Actuators B Chem 285:385. https://doi.org/10.1016/j.snb.2019.01.076
101. Guo W, Qi X, Orbach R, Lu C, Freage L, Mironi-Harpaz I, Seliktar D, Yang H-H, Willner I (2014) Chem Commun 50:4065. https://doi.org/10.1039/C3CC49140D
102. Yu X, Hu Y, Kahn JS, Cecconello A, Willner I (2016) Chemistry 22:14504. https://doi.org/10.1002/chem.201603653
103. Li J, Yu J, Huang Y, Zhao H, Tian L (2018) ACS Appl Mater Interfaces 10:26075. https://doi.org/10.1021/acsami.8b09152

104. Geng J, Yao C, Kou X, Tang J, Luo D, Yang D (2018) Adv Healthc Mater 7:1700998. https://doi.org/10.1002/adhm.201700998
105. Famulok M, Hartig JS, Mayer G (2007) Chem Rev 107:3715. https://doi.org/10.1021/cr0306743
106. Yang H, Liu H, Kang H, Tan W (2008) J Am Chem Soc 130:6320. https://doi.org/10.1021/ja801339w
107. Wang Z, Xia J, Cai F, Zhang F, Yang M, Bi S, Gui R, Li Y, Xia Y (2015) Colloids Surf B Biointerfaces 134:40. https://doi.org/10.1016/j.colsurfb.2015.06.031
108. Zhu Z, Wu C, Liu H, Zou Y, Zhang X, Kang H, Yang CJ, Tan W (2010) Angew Chem Int Ed Engl 49:1052. https://doi.org/10.1002/anie.200905570
109. Zhou L, Chen C, Ren J, Qu X (2014) Chem Commun 50:10255. https://doi.org/10.1039/c4cc04791e
110. Liu R, Huang Y, Ma Y, Jia S, Gao M, Li J, Zhang H, Xu D, Wu M, Chen Y, Zhu Z, Yang C (2015) ACS Appl Mater Interfaces 7:6982. https://doi.org/10.1021/acsami.5b01120
111. Ma Y, Mao Y, Huang D, He Z, Yan J, Tian T, Shi Y, Song Y, Li X, Zhu Z, Zhou L, Yang CJ (2016) Lab Chip 16:3097. https://doi.org/10.1039/c6lc00474a
112. Iwasaki Y, Kondo J, Kuzuya A, Moriyama R (2016) Sci Technol Adv Mater 17:285. https://doi.org/10.1080/14686996.2016.1189798
113. Yan L, Zhu Z, Zou Y, Huang Y, Liu D, Jia S, Xu D, Wu M, Zhou Y, Zhou S, Yang CJ (2013) J Am Chem Soc 135:3748. https://doi.org/10.1021/ja3114714
114. Zhu Z, Guan Z, Jia S, Lei Z, Lin S, Zhang H, Ma Y, Tian ZQ, Yang CJ (2014) Angew Chem Int Ed Engl 53:12503. https://doi.org/10.1002/anie.201405995
115. Wei X, Tian T, Jia S, Zhu Z, Ma Y, Sun J, Lin Z, Yang CJ (2015) Anal Chem 87:4275. https://doi.org/10.1021/acs.analchem.5b00532
116. Tian T, Wei X, Jia S, Zhang R, Li J, Zhu Z, Zhang H, Ma Y, Lin Z, Yang CJ (2016) Biosens Bioelectron 77:537. https://doi.org/10.1016/j.bios.2015.09.049
117. Liu D, Jia S, Zhang H, Ma Y, Guan Z, Li J, Zhu Z, Ji T, Yang CJ (2017) ACS Appl Mater Interfaces 9:22252. https://doi.org/10.1021/acsami.7b05531
118. Ma Y, Mao Y, An Y, Tian T, Zhang H, Yan J, Zhu Z, Yang CJ (2018) Analyst 143:1679. https://doi.org/10.1039/c8an00010g
119. Li Y, Ma Y, Jiao X, Li T, Lv Z, Yang CJ, Zhang X, Wen Y (2019) Nat Commun 10:1036. https://doi.org/10.1038/s41467-019-08952-1
120. Yin B, Ye B, Wang H, Zhu Z, Tan W (2012) Chem Commun 48:1248. https://doi.org/10.1039/C1CC15639J
121. Zhang L, Lei J, Liu L, Li C, Ju H (2013) Anal Chem 85:11077. https://doi.org/10.1021/ac4027725
122. Zhou L, Sun N, Xu L, Chen X, Cheng H, Wang J, Pei R (2016) RSC Adv 6:114500. https://doi.org/10.1039/c6ra23462c
123. Simon AJ, Walls-Smith LT, Freddi MJ, Fong FY, Gubala V, Plaxco KW (2017) ACS Nano 11:461. https://doi.org/10.1021/acsnano.6b06414
124. Simon AJ, Walls-Smith LT, Plaxco KW (2018) Analyst 143:2531. https://doi.org/10.1039/c8an00337h
125. Liu H, Cao T, Xu Y, Dong Y, Liu D (2018) Int J Mol Sci 19:1633. https://doi.org/10.3390/ijms19061633
126. Yang Z, Zhuo Y, Yuan R, Chai Y (2017) Nanoscale 9:2556. https://doi.org/10.1039/c6nr08353f
127. Liu C, Han J, Pei Y, Du J (2018) Appl Sci Basel 8:1941. https://doi.org/10.3390/app8101941
128. Li J, Zheng C, Cansiz S, Wu C, Xu J, Cui C, Liu Y, Hou W, Wang Y, Zhang L, Teng I, Yang H, Tan W (2015) J Am Chem Soc 137:1412. https://doi.org/10.1021/ja5122931
129. Chen F, Bai M, Cao K, Zhao Y, Cao X, Wei J, Wu N, Li J, Wang L, Fan C, Zhao Y (2017) ACS Nano 11:11908. https://doi.org/10.1021/acsnano.7b06728
130. Chen F, Bai M, Zhao Y, Cao K, Cao X, Zhao Y (2018) Anal Chem 90:2271. https://doi.org/10.1021/acs.analchem.7b04634
131. McGhee CE, Loh KY, Lu Y (2017) Curr Opin Biotechnol 45:191. https://doi.org/10.1016/j.copbio.2017.03.002
132. Lin H, Zou Y, Huang Y, Chen J, Zhang WY, Zhuang Z, Jenkins G, Yang CJ (2011) Chem Commun (Camb) 47:9312. https://doi.org/10.1039/c1cc12290h
133. Huang Y, Ma Y, Chen Y, Wu X, Fang L, Zhu Z, Yang CJ (2014) Anal Chem 86:11434. https://doi.org/10.1021/ac503540q
134. Mao Y, Li J, Yan J, Ma Y, Song Y, Tian T, Liu X, Zhu Z, Zhou L, Yang C (2017) Chem Commun 53:6375. https://doi.org/10.1039/c7cc01360d

135. Huang Y, Fang L, Zhu Z, Ma Y, Zhou L, Chen X, Xu D, Yang C (2016) Biosens Bioelectron 85:496. https://doi.org/10.1016/j.bios.2016.05.008
136. Lilienthal S, Shpilt Z, Wang F, Orbach R, Willner I (2015) ACS Appl Mater Interfaces 7:8923. https://doi.org/10.1021/acsami.5b02156
137. Kang H, Liu H, Zhang X, Yan J, Zhu Z, Peng L, Yang H, Kim Y, Tan W (2011) Langmuir 27:399. https://doi.org/10.1021/la1037553
138. Shimomura S, Nishimura T, Ogura Y, Tanida J (2018) R Soc Open Sci 5:171779. https://doi.org/10.1098/rsos.171779
139. Dirks RM, Pierce NA (2004) Proc Natl Acad Sci 101:15275. https://doi.org/10.1073/pnas.0407024101
140. Bi S, Yue SZ, Zhang SS (2017) Chem Soc Rev 46:4281. https://doi.org/10.1039/c7cs00055c
141. Wang J, Chao J, Liu H, Su S, Wang L, Huang W, Willner I, Fan C (2017) Angew Chem Int Ed Engl 56:2171. https://doi.org/10.1002/anie.201610125
142. Song P, Ye D, Zuo X, Li J, Wang J, Liu H, Hwang MT, Chao J, Su S, Wang L, Shi J, Wang L, Huang W, Lal R, Fan C (2017) Nano Lett 17:5193. https://doi.org/10.1021/acs.nanolett.7b01006
143. Li D, Song S, Fan C (2010) Acc Chem Res 43:631. https://doi.org/10.1021/ar900245u
144. Xue J, Chen F, Bai M, Yu X, Wei J, Huang P, Zhao Y (2017) ChemNanoMat 3:725. https://doi.org/10.1002/cnma.201700177
145. Zhao Y, Chen F, Qin J, Wei J, Wu W, Zhao Y (2018) Chem Sci 9:392. https://doi.org/10.1039/C7SC03994H
146. Li J, Fan C, Pei H, Shi J, Huang Q (2013) Adv Mater 25:4386. https://doi.org/10.1002/adma.201300875
147. Pei H, Zuo X, Zhu D, Huang Q, Fan C (2014) Acc Chem Res 47:550. https://doi.org/10.1021/ar400195t
148. Yang F, Zuo X, Fan C, Zhang X-E (2018) Natl Sci Rev 5:740. https://doi.org/10.1093/nsr/nwx134
149. Ye D, Zuo X, Fan C (2018) Annu Rev Anal Chem 11:171
150. Ge Z, Li Q, Fan C (2019) Chem Res Chin Univ 36:1. https://doi.org/10.1007/s40242-019-9249-4
151. Hu Q, Li H, Wang L, Gu H, Fan C (2019) Chem Rev 119:6459. https://doi.org/10.1021/acs.chemrev.7b00663
152. Song S, Qin Y, He Y, Huang Q, Fan C, Chen H (2010) Chem Soc Rev 39:4234. https://doi.org/10.1039/c000682n
153. Chen N, Li J, Song H, Chao J, Huang Q, Fan C (2014) Acc Chem Res 47:1720. https://doi.org/10.1021/ar400324n
154. Jia S, Chao J, Fan C, Liu H (2014) Prog Chem 26:695. https://doi.org/10.7536/pc140130
155. Liu X, Zhao Y, Liu P, Wang L, Lin J, Fan C (2019) Angew Chem Int Ed Engl 58:8996. https://doi.org/10.1002/anie.201807779
156. Wang F, Zhang X, Liu X, Fan C, Li Q (2019) Small 15:1900013. https://doi.org/10.1002/smll.201900013
157. Zhao Y, Dai X, Wang F, Zhang X, Fan C, Liu X (2019) Nano Today 26:123. https://doi.org/10.1016/j.nantod.2019.03.004
158. Wu N, Chen F, Zhao Y, Yu X, Wei J, Zhao Y (2018) Langmuir 34:14721. https://doi.org/10.1021/acs.langmuir.8b01818